Transportation Research Part B 99 (2017) 138–166

Contents lists available at ScienceDirect

Transportation Research Part B

journal homepage: www.elsevier.com/locate/trb

# Network user equilibrium problems for the mixed battery electric vehicles and gasoline vehicles subject to battery swapping stations and road grade constraints

Min Xu[a], Qiang Meng[a,*], Kai Liu[b]

[a] Department of Civil and Environmental Engineering, National University of Singapore, Singapore 117576, Singapore
[b] School of Transportation and Logistics, Dalian University of Technology, Dalian 116024, PR China

ARTICLE INFO

*Article history:*
Received 14 August 2016
Revised 20 November 2016
Accepted 18 January 2017
Available online 31 January 2017

*Keywords:*
User equilibrium
Battery electric vehicles
Battery swapping stations
Road grade
Flow-dependent electricity consumption

ABSTRACT

There has been growing attention on battery electric vehicles (BEVs) due to their energy efficiency and environmental friendliness. This paper deals with the user equilibrium (UE) problems for the mixed BEVs and traditional gasoline vehicles (GVs) in transportation networks with battery swapping stations and road grade constraints. Under the assumption that electricity consumption rate is not affected by traveling speed or traffic flow, a nonlinear minimization model in terms of path flows is first formulated by incorporating effects of road grade on the electricity consumption rate. The battery swapping action based paths are defined for BEVs in the represented network to facilitate the model building with flow-dependent dwell time at the battery swapping stations. The Frank-Wolfe (F-W) algorithm, where descent direction is found by the multi-label method in a pseudo-polynomial time, is adopted to solve the model. Moreover, the aforementioned assumption about the flow-independent electricity consumption rate is then relaxed and a system of inequalities has been proposed to formulate the UE conditions. For the nonlinear minimization model, two numerical examples are presented to assess the propose model and algorithm, as well as to analyze the impact of usable battery capacity, BEVs' market share and some attributes of battery swapping stations on the equilibrium link flows and/or swapping flows. The system of inequalities is exactly solved for a small network by path enumeration to demonstrate the non-uniqueness of UE link flow solutions.



## 1. Introduction

Compared with the conventional gasoline vehicles (GVs), the battery electric vehicles (BEVs) deliver many benefits like low greenhouse gas (GHG) emission and high energy efficiency (Berr, 2008; Duvall, 2007). Plug-in charging and battery swapping are two prevailing technologies for BEVs to get a depleted battery refreshed. The former one recharges BEVs at home or charging stations and the latter replaces a depleted battery with a fully charged one at the battery swapping stations. The scarce charging infrastructure and long charging time, however, hinder the adoption of BEVs on a mass scale (Charles Botsford, 2009). The limited driving range of fully-charged BEVs further reduces public incentive to purchase BEVs because they have to frequently recharge their BEVs during a long journey. To address this issue, more charging stations or battery swapping stations have to be deployed in a transportation network.

* Corresponding author.
*E-mail address:* ceemq@nus.edu.sg (Q. Meng).

http://dx.doi.org/10.1016/j.trb.2017.01.009
0191-2615/

The routing behaviors of BEV drivers in a transportation network with battery charging and swapping stations are essentially different. Although under both circumstances, the drivers select the efficient routes to reach the charging or swapping stations if they are in need of charging/swapping, the tradeoff between charging time and charging amount should be balanced exclusively at the battery charging stations. In reality, battery swapping is equivalent to charging a predefined amount of electricity at the battery charging stations from the aspect of modeling, where the charging amount is pre-specified parameter known by drivers rather than a decision variable made by them.

Typically, a fast changing station takes about 35 min to replenish a depleted battery of 35 kW h even with a power level as high as 60 kW (ETEC, 2010), whereas the BEV drivers may exchange their depleted battery within two or three minutes at a swapping station (Mak et al., 2013). In other words, the battery swapping is more efficient than battery charging in terms of the time to replenish energy. This advantage has made BEVs comparable to GVs since the time to swap the battery of a BEV is almost the same with or even less than the time to fill the tank of a GV. In addition, batteries with highest energy density (potentially with longest driving range) are promising candidates for battery swapping due to their unique process to get replenished (EC, 2007). Moreover, as elaborated previously, battery swapping is equivalent to charging a BEV fully or for a predefined amount of electricity. With the great improvements in science and technology, advanced batteries with higher energy density and charging methods with less charging time may come to the market in the foreseeable future. For example, researchers from Singapore have developed an ultra-fast charging battery which can get 70% of its battery capacity recharged in only two minutes (NTU, 2014). Once this technology becomes mature, there would be almost no difference between battery charging and swapping stations because drivers would charge their batteries fully considering the negligible charging time. Hence, this study aims to model the user equilibrium (UE) behaviors of BEVs in their route choice with the battery swapping stations.

Given the long charging time, limited driving range and charging infrastructure, both BEVs and GVs will coexist in the transportation networks for a long time. The behaviors of BEV and GV drivers in their route choice from an origin to a destination are distinct because the BEV drivers have to exchange batteries at the battery swapping stations during their journeys. In addition, the fear of running out of electricity before reaching their destinations or battery swapping stations, referred to as *range anxiety* (Eberle and von Helmolt, 2010; Pearre et al., 2011), will make their route choice decision process more complicated. It is well recognized that road grade has significant impact on the energy consumption of BEVs (Frey et al., 2008; Liu et al., 2015; Travesset-Baro et al., 2015) and more electricity will be consumed on a road with steep upslope and vice versa. As a result, the road grade will inevitably affect the driving range, the range anxiety and route choice in turn for BEVs. This study, therefore, focuses on model development and algorithm design for the UE problems in a transportation network running both BEVs and GVs subject to the battery swapping station and road grade constraints.

### 1.1. Literature review

UE problem is a fundamental and important problem for transportation planning. It aims to predict the traffic flow under the assumption that all the travelers make their route choice by selecting the path with minimal travel cost (Wardrop, 1952). Apart from its wide application in road congestion pricing (Yang and Huang, 2005; Meng et al., 2012), network design problems (Yang and Bell, 1998; Wang et al., 2013; Ban et al., 2006) etc., over the past decades, researchers have made several extensions by relaxing the aforementioned assumption and incorporating more realism into the traditional UE. The prominent examples include the stochastic user equilibrium (SUE) (Daganzo and Sheffi, 1977; Meng and Liu, 2012) and boundedly rational user equilibrium (BRUE) (Di et al., 2013; Di and Liu, 2016; Lou et al., 2010). Most of these studies focused on the UE problem of GVs. As for BEVs, Jing et al. (2016) have recently provided a comprehensive review for the network modeling of BEVs, where UE problem with BEVs is particularly discussed. In view of the focus of this study, we only review the relevant studies on the UE problems with BEVs. The other studies, including the BEV touring, routing and scheduling problems (Liao et al., 2016; Adler et al., 2016; Adler and Mirchandani, 2014; Schneider et al., 2014), the market penetration and climate impact analysis of BEVs (Egbue and Long, 2012; Yabe et al., 2012) and the optimal deployment of recharging or swapping stations (He et al., 2013; Mak et al., 2013; Nie and Ghamami, 2013; Sathaye and Kelley, 2013; He et al., 2015; Ghamami et al., 2016; Li et al., 2016), will not be covered by the literature review presented below.

Jiang et al. (2012), Jiang et al. (2014) and Jiang and Xie (2014) proposed three distance-constrained UE models for the transportation networks running both BEVs and GVS without the charging station constraint under different problem settings. They applied the Frank–Wolfe (F–W) method, projected gradient method, and the partial linearization method incorporating with a special weight constrained shortest path problem (WCSPP) for solving their distance-constrained UE models. To be more specific, Jiang et al. (2012) put forward a Frank–Wolfe method with the label-setting method solving the WCSPP (FW-WCSPP) for the distance-constrained UE model. Jiang and Xie (2014) used the Frank–Wolfe algorithmic framework with a modified one-to-all label-setting method (FW-MLS) as well as the projected gradient method with a combined preprocessing and label-setting method (PG-PLS) respectively, for solving the combined UE model with distance constraints. They later employed the partial linearization method with a combined pre-processing and label-setting method (PLM-PLS) to solve another combined and distance-constrained UE model.

The number of aforementioned studies made by Jiang and his research collaborators does not take into account locations of charging or swapping stations over a network. He et al. (2014) made the first attempt to investigate the UE problem with the plug-in charging stations, where BEV drivers decide where and how much to charge their BEVs. They built a convex programming model for the UE problem when the recharging time are considered and developed an iterative algorithm for

**Table 1**
Main features of the existing studies on the UE for BEVs.

| Study | Problem setting | Model | Solution algorithm | Vehicles | Test examples | Stations | Road Grade |
|---|---|---|---|---|---|---|---|
| Jiang et al. (2012) | UE with distance constrains | Distance-constrained network equilibrium convex programming model | FW-WCSPP | GVs & BEVs | Sioux Falls | No | No |
| Jiang & Xie (2014) | UE with mode & route choice | Combined network equilibrium convex programming model with distance constrains | FW-MLS; PG-PLS | GVs & BEVs | Nguyen-Dupuis; Sioux Falls; Anaheim | No | No |
| Jiang et al., (2014) | UE with destination, route & parking choice | Combined Network equilibrium convex programming model with distance constrains | PLM-PLS | GVs & BEVs | Lam-Huang; Anaheim | No | No |
| He et al. (2014) | UE | Network equilibrium convex programming models | CONOPT/PATH-CPLEX 12.2 | BEVs | Nguyen-Dupuis; Sioux Falls | Plug-in Charging stations | No |

solving their models. The sub-problem of their algorithm is a mixed integer linear problem to be solved by CPLEX 12.2 for small and medium instances. However, due to the NP-hardness of the mixed integer linear programming, their algorithm may not be efficient for the implementation in the large-scale networks.

Table 1 summarizes the main features of the existing studies on the UE problems for BEVs. It shows that the existing studies mainly focus on the plug-in charging behavior of BEVs and little attention has been paid to the adoption of the battery swapping technology. Although the battery swapping scheme seems hard to implement in practice at present both for its high cost, it have many advantages compared with the recharging strategy for its negligible time to replenish electricity. Besides, with the development of battery technology, there will be no difference between battery charging and swapping stations because drivers charge their battery fully due to the negligible charging time. It is therefore of great importance to investigate the UE behaviors of BEV drivers in their route choice from an origin to a destination in the transportation networks with the battery swapping stations.

In addition, the existing relevant studies have not considered the impact of road grade on the electricity consumption rate (kW h/km) of BEVs. Unlike GVs, BEVs can store the regenerative braking energy (Chan, 2007), and it is obvious that more energy will be saved on a road with the steep downslope and vise verse. The road grade therefore inevitably alters the driving range, affects the range anxiety and ultimately influences route choice of BEV drivers. Over the past years, a few researchers have advocated the impact of road grade on energy consumption efficiency (Frey et al., 2008; Liu et al., 2015; Travesset-Baro et al., 2015). Liu et al. (2015) developed eight regression models using the operational data of 495 BEVs in Japan. Their results showed that the adjusted goodness of estimated electric consumption efficiency model will increase when the percentage of road length for different road grade is considered as an extra explanatory variable. From the estimated parameters of the linear energy consumption efficiency model [Model 4 in (Liu et al., 2015)], more remarkable effect on energy consumption efficiency was observed on steeper road profile both in upward and downward slopes, and more electricity will be consumed in upslope than saved in downslope of same road grade. Presumably, BEV drivers will choose a path with steeper downslope and more flat upslope among all the paths with the same travel time. However, the effect of road grade on the electricity consumption rate of BEVs has been ignored in the existing studies on the UE problem. Assuming a flat road profile rather than a gradient one may cause discrepancy in real-world driving range, it is thus important to reveal the drivers' behaviors considering the effects of road grade on electricity consumption rate of BEVs. Although energy consumption efficiency of GVs is also affected by road grade than that of BEV (Travesset-Baro et al., 2015), it is assumed that range anxiety is not applied to drivers of GVs since the driving range of GV is generally much larger than BEV.

It is practical that queues may arise at a battery swapping station when the swapping BEV flows exceed a threshold (i.e., capacity). The dwell time for BEV in the swapping stations may be substantial even if the free-flow swapping time may be negligible. Moreover, efficient and convenient as it is, the battery swapping activity may be too expensive that the BEV drivers will not swap a battery unless necessary. For example, according to the authorities of Tesla Motors, a battery swapping will cost about $60 to $80 (Zhang, 2015). Considering the value of time as $20per h, swapping a battery is equivalent to spending three to four hour during their journeys. It is thus reasonable to incorporate the effect of dwell time and swapping cost at a battery swapping station on the UE modeling with BEVs. In this regard, the BEV drivers would like to choose the shortest feasible path along which the battery swapping stations with less congestion are visited only if necessary.

Although the adaptation of the battery swapping strategy makes BEVs comparable to GV in terms of time to replenish energy, there will be a long time that both types of vehicles coexist in the transportation networks. With the interaction of BEVs and GVs, the route choice behavior of drivers will become more complicated and the UE flows of BEVs and GVs will be

quite different. To the best of our knowledge, no research about UE problem for the mixed BEVs and GVs in a transportation network with battery swapping stations and road grade constraints has been done before. The literature review on the existing studies on the UE problem of BEVs fully reveals the merits of the UE models and algorithms proposed by this study.

### 1.2. Objectives and contributions

The objective of this study is to develop mathematical models and design solution methods for the UE problems BEVs and GVs by taking into account the battery swapping stations and road grade constraints. For BEVs, several algorithms were proposed to solve the vehicle routing problems (VRP) whose objective is to find the shortest path for a BEV under specific constraints. For example, the electric vehicle shortest walk problem with swapping station (EV-SWP) has been formulated by Adher et al. (2014). Their polynomial-time algorithm relays on the assumption that the fuel and length components of each link are constant and equal. Schneider et al. (2014) proposed a hybrid heuristic to solve the electric vehicle routing problem with time windows. In addition, the shortest path problem of BEV with swapping stations, referred to as the shortest battery swapping action based path problem (SBSAPP) is closely related to other problems that have received a significant amount of attention in the literature. For example, WCSPP is a special case of SBSAPP when there are no swapping stations in the networks. WCSPP can be solved efficiently by preprocessing, labeling and scaling algorithms in practice (Aneja et al., 1983; Dumitrescu and Boland, 2003). When taking the swapping stations into consideration, WCSPP is transformed to be SBSAPP. To the best of our knowledge, only a few studies considered relay or replenishment in the context of WCSPP (Cabral, 2005; Laporte and Pascoal, 2011; Smith et al., 2012), among which the algorithms for minimum cost path problem with relays (MCPPR) developed by Laporte and Pascoal (2011) shows very promising results in computational time. In this paper, the multi-label method for solving the shortest battery swapping action based path problem (ML-SBSAPP), as an improved version of an existing algorithm solving MCPPR, is proposed to solve the sub-problem of the F–W algorithm in a pseudo-polynomial time.

In all, the contributions of this study are multidimensional. First, we make the first attempt to investigate the drivers' behavior of BEV and GV in a transportation network with swapping stations, which is different from previous models with charging stations or no stations at all. The effects of road grade on the electricity consumption rate of BEVs and the impact of queue arising in swapping stations on the equilibrium BEV flows are also explicitly incorporated in the proposed models. Second, a Frank–Wolfe (F–W) algorithmic framework with ML-SBSAPP is proposed to solve the model, which is computationally efficient and have the potential to be applied in real networks. Third, we show that the there are some flaws for the UE conditions with charging stations when electricity consumption rate is flow-dependent. A set of new UE conditions in the context of mixed BEVs and GVs with battery swapping stations and road grade constraints are presented and discussed.

The remainder of this paper is organized as follows. First, assumptions, notations and the UE problem are elaborated in Section 2. Under the assumption that electricity consumption rate of BEVs is not affected by traveling speed (flow-independent electricity consumption rate), Section 3 develops a UE model for the mixed BEVs and GVs with battery swapping stations and road grade constraints. To solve the developed UE model, a F–W algorithmic framework is proposed and details are presented for the multi-label method for solving SBSAPP in Section 4. Section 5 relaxes the aforementioned assumption by assuming that the electricity consumption rate of BEV depends on the traveling speed/traffic flow and a system of inequalities have been formulated to represent the correspondent UE conditions. Results of some numerical examples are provided in Section 6. Conclusions and future research are presented in Section 7. Appendix lists the abbreviations and notations used in this paper for readability.

## 2. Assumptions, notations and UE conditions with mixed BEVs and GVs

Consider a transportation network running both BEVs and GVs with battery swapping stations and road grade, denoted by $G=(N, A)$ where $N$ is the set of nodes and $A$ is the set of links. The sets of origins and destinations are denoted by $R\subseteq N$ and $S\subseteq N$, respectively. Without loss of generality, it is assumed that each link $a$: $=(i, j) \in A$, $i, j \in N$ with the length of $l_a$ kilometres has only one road grade denoted by $g_a$, and that a battery swapping station is located in a particular node. All the battery swapping stations are grouped into a set denoted by $I\subset N$. The usable battery capacities for BEVs are not necessarily the same in practice. Hence, all the BEVs are divided into different groups, denoted by the set $M$, in terms of their usable battery capacity. In other words, each BEV in group $m \in M$ has the same usable battery capacity denoted by $W_m$ (kWh). Additionally, it is reasonable to assume that the battery swapping cost is the same for all the swapping stations but different for various BEVs groups. Let $\lambda_m$ (S$) be the battery swapping cost at a battery swapping station for BEVs in the group $m \in M$. For simplicity, it is assumed that the initial amount of electricity in the battery of all BEVs in the group $m \in M$ originating from their origins, denoted by $W_m^0$, is equal to the correspondent usable battery capacity, namely, $W_m^0 = W_m$. It is further assumed that all the BEV and GV drivers have the same value of time (VOT), denoted by $\tau$.

Let $q_{e,m}^{rs}$ and $q_g^{rs}$ be the travel demands of BEVs in group $m \in M$ and GVs between O–D pair $(r, s)$ respectively, where $r \in R$ and $s \in S$. Let $x_a$ denote the aggregated traffic flow on link $a \in A$comprising the GV flow denoted by $x_{ag}$and the BEV flow denoted by $x_{ae}$. The aggregated BEV battery swapping flow at the battery swapping station $i \in I$ is denoted by $y_i$, comprising the battery swapping flow of BEVs in each group, namely: $y_i = \sum_{m\in M} y_{i,m}$. Let us first assume that the electricity consumed

by a BEV traveling on link $a \in A$, denoted by $w_a$ (kW h), depends on the length and grade of the link, namely:

$$w_a = \phi(l_a, g_a) \tag{1}$$

where $\phi(l_a, g_a)$ is an given electricity consumption function with respect to length $l_a$ and grade $g_a$. The value of electricity consumption for a single link can be negative due to the energy saving from regenerative braking, especially on a road with the steep downslope. The function $\phi(l_a, g_a)$ can be established by the regression analysis methods using the real or experimental data. It should be pointed out that the electricity consumption of BEVs on a link may depend on the flow-dependent travel time (i.e. travel speed) in addition to the travel distance and road grade, the flow-independent electricity consumption function shown in Eq. (1) will be relaxed in the latter of this study.

### 2.1. Battery swapping action based feasible paths

Let $K_g^{rs}$ denote the set of all the physical paths from an origin $r$ to a destination $s$ in the network $G=(N, A)$ for GVs. Here, a physical path may contain cycles and any cycle on the path can appear at most once. In other words, a physical path may not be a simple path. Any physical path $p \in K_g^{rs}$ can be represented by a sequence of visiting nodes, namely:

$$p := v_1 \to v_2 \to \cdots v_{l-1} \to v_l \tag{2}$$

where $l$ is the number of nodes on the path, and $v_1=r, v_l=s$ and $v_i \in N$, $i=2, 3, \cdots, l-1$. Alternatively, it can be represented by a series of links, namely:

$$p := \{(v_i, v_{i+1}) | (v_i, v_{i+1}) \in A, i = 1, 2, \ldots, l-1\} \tag{3}$$

The electricity consumption of a BEV on path $p$ expressed by Eqs. (2) or (3) can be calculated by

$$w[p] = \sum_{i=1}^{l-1} w_{v_i v_{i+1}} = \sum_{a \in p} w_a \tag{4}$$

Let $\sigma_p(v_i, v_j)$ denote the sub-path of path $p$from nodes $v_i$ to $v_j$, namely:

$$\sigma_p(v_i, v_j) := v_i \to v_{i+1} \to \cdots \to v_j \tag{5}$$

or

$$\sigma_p(v_i, v_j) := \{(v_k, v_{k+1}) | (v_k, v_{k+1}) \in A, k = i, \ldots, j-1\} \tag{6}$$

The electricity consumption of a BEV on the sub-path $\sigma_p(v_i, v_j)$ can be computed by

$$w[\sigma_p(v_i, v_j)] = \sum_{k=i}^{j-1} w_{v_k v_{k+1}} = \sum_{a \in \sigma_p(v_i, v_j)} w_a \tag{7}$$

A feasible path for a GV from an origin to a destination may be infeasible for a BEV due to the limited usable battery capacity. One feasible path for GV with several battery swapping stations along it can be formulated as several different feasible paths with the battery swapping actions for BEV. Hence, a path incorporating the battery swapping actions is referred to as a *battery swapping action based path* (BSAP) for BEVs to distinguish it from the physical path used by GVs. All the BSAPs of BEVs can be generated from the physical paths of GVs according to whether a battery swapping action is taken by the BEV drivers at each battery swapping station. Therefore, a single physical path with $L$ battery swapping stations can generate $2^L$ BSAPs in total by enumerating all the possible combinations of battery swapping actions along that physical path. However, some of these BSAPs may be infeasible for BEVs. Nevertheless, the set of all the feasible BSAPs for BEVs generated from the finite physical paths can be pre-determined.

Assume that there are $L_p > 0$ battery swapping stations located in the nodes of the physical path $p$ expressed by Eq. (2) or (3) from an origin $r$ to a destination$s$. These battery swapping stations are denoted by their visiting sequences (nodes) on the path: $v_{i_1}, v_{i_2}, \ldots, v_{i_{L_p}}$, where $v_{i_k} \in \{v_2, v_3, \ldots, v_{l-1}\}$ and $i_1 < i_2 < \cdots < i_{L_p}$. With respect to the physical path$p$, a BSAP with $h$ battery swapping actions at the nodes denoted by $\hat{v}_{j_1}, \hat{v}_{j_2}, \ldots, \hat{v}_{j_h}$, where $\hat{v}_{j_k} \in \{v_{i_1}, v_{i_2}, \ldots, v_{i_{L_p}}\}, k = 1, 2, \ldots, h$, and $j_1 < j_2 < \cdots < j_h$, is feasible for the BEV in the group $m \in M$ if and only if:

$$w[\sigma_p(r, \hat{v}_{j_1})] \le W_m^0 \tag{8}$$

$$w[\sigma_p(\hat{v}_{j_k}, \hat{v}_{j_{k+1}})] \le W_m (k = 1, 2, \ldots, h-1) \tag{9}$$

$$w[\sigma_p(\hat{v}_{j_h}, s)] \le W_m \tag{10}$$

For each BSAP of BEVs, given that $W_m^0 = W_m$, we define the *inter-swapping sub-paths* as the sub-paths between two adjacent swapping stations with battery swapping actions or sub-path between origin/destination and nearest swapping stations

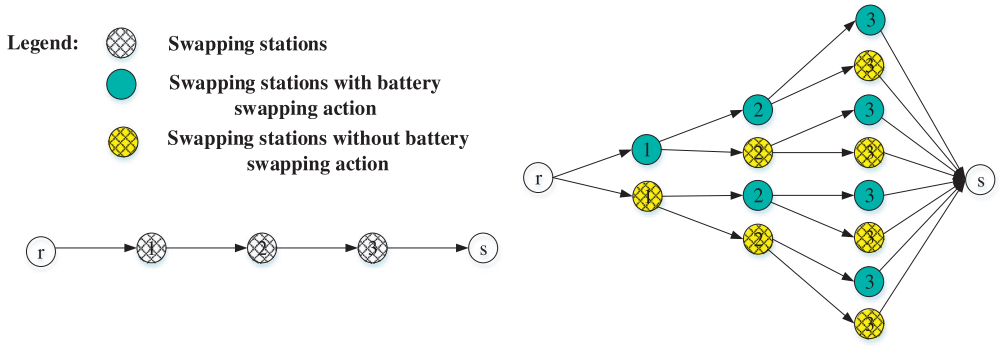


**Fig. 1.** An example for the BSAP generation.

with battery swapping actions. Eqs. (8)–(10) imply that the amount of electricity consumed by a BEV on all the inter-swapping sub-paths should not exceed the usable capacity of a battery. The path $p$ is feasible for BEVs without any battery swapping actions provided that

$$w[p] \le W_m^0 \tag{11}$$

Let $K_{e,m}^{rs}$ denote the set of all the feasible BSAPs for BEVs in the group $m \in M$ from origin $r$ to destinations, namely:

$$\begin{aligned} K_{e,m}^{rs} = &\left\{ w[p] \le W_m^0, \forall p \in K_g^{rs} \right\} \cup \left\{ \sigma_p(r, \hat{v}_{i_1}) \oplus \sigma_p(\hat{v}_{i_j}, \hat{v}_{i_{j+1}}) \oplus \sigma_p(\hat{v}_{i_h}, s), \forall p \in K_g^{rs} \middle| \right. \\ &\left. w[\sigma_p(r, \hat{v}_{i_1})] \le W_m^0 \& w[\sigma_p(\hat{v}_{i_j}, \hat{v}_{i_{j+1}})] \le W_m (j = 1, 2, \ldots, h-1) \& w[\sigma_p(\hat{v}_{i_h}, s)] \le W_m \right\} \end{aligned} \tag{12}$$

where operator $\oplus$ denotes the concatenation of two sub-paths.

We now use an example to illustrate how to pre-determine the set of BSAPs for BEVs. It is assumed that the physical path from origin $r$ to destination $s$ shown in the part (a) of Fig. 1 has three battery swapping stations, namely nodes 1, 2 and 3. Hence, there are eight ($2^3$) possible combinations of battery swapping actions for a BEV traveling on this physical path and they can be represented by the eight BSAPs depicted in the part (b) of Fig. 1. For instance, path $p := r \to \hat{1} \to 2 \to \hat{3} \to s$ codes a BSAP for BEV on which the BEV drivers will swap a battery at stations 1 and 3 respectively. Moreover, if $w[\sigma_p(r, \hat{1})] \le W_m^0$, $w[\sigma_p(\hat{1}, \hat{3})] \le W_m$ and $w[\sigma_p(\hat{3}, s)] \le W_m$, then the path $p$ is a feasible BSAP from origin $r$ to destination $s$ for BEVs in group $m \in M$.

### 2.2. BEV flow at a battery swapping station and overall flow conservation equations

For O–D pair $(r, s)$, $f_{k_g}^{rs}$ represents the traffic flow of GVs on path $k_g \in K_g^{rs}$, whereas $f_{k_e^m}^{rs}$ denotes the flow of BEVs in the group $m \in M$ on the feasible BSAP $k_e^m \in K_{e,m}^{rs}$. The path flows and link flows of BEVs and GVs should fulfill the fundamental flow conservation equations:

$$\sum_{k_g \in K_g^{rs}} f_{k_g}^{rs} = q_g^{rs}, \forall r \in R, s \in S \tag{13}$$

$$\sum_{k_e^m \in K_{e,m}^{rs}} f_{k_e^m}^{rs} = q_{e,m}^{rs}, \forall r \in R, s \in S, m \in M \tag{14}$$

$$f_{k_g}^{rs} \ge 0, f_{k_e^m}^{rs} \ge 0, \forall r \in R, s \in S, k_g \in K_g^{rs}, k_e^m \in K_{e,m}^{rs} \tag{15}$$

Based on these path flows, the mixed traffic flow on a link and the BEV swapping flow at a battery swapping station can be calculated by

$$x_a = x_{ag} + x_{ae}, \forall a \in A \tag{16}$$

$$y_i = \sum_{m \in M} y_{i,m}, \forall i \in I \tag{17}$$

where

$$x_{ag} = \sum_{r \in R} \sum_{s \in S} \sum_{k_g \in K_g^{rs}} f_{k_g}^{rs} \delta_{a,k_g}^{rs}, \forall a \in A \tag{18}$$

$$x_{ae} = \sum_{r\in R}\sum_{s\in S}\sum_{m\in M}\sum_{k_e^m\in K_{e,m}^{rs}} f_{k_e^m}^{rs}\delta_{a,k_e^m}^{rs}, \forall a \in A \tag{19}$$

$$y_{i,m} = \sum_{r\in R}\sum_{s\in S}\sum_{k_e^m\in K_{e,m}^{rs}} f_{k_e^m}^{rs}\delta_{i,k_e^m}^{rs}, \forall i \in I, m \in M \tag{20}$$

in which $\delta_{a,k_g}^{rs}$ is the path-link incidence indicator for GVs, which equals 1 if path $k_g$ traverses link $a$ and 0 otherwise; $\delta_{a,k_e^m}^{rs}$ is the BSAP-link incidence indicator for BEVs in the group $m \in M$, which equals 1 if the feasible BSAP $k_e^m$ traverses link $a$ and 0 otherwise; $\delta_{i,k_e^m}^{w}$ is the BSAP-swapping action incidence indicator which equals 1 if the feasible BSAP $k_e^m$ traverses the swapping station $i \in I$ where a battery swapping action is taken and 0 otherwise.

### 2.3. User equilibrium conditions

The travel time function of link $a$: $=(i, j) \in A$ is denoted by $t_a(x_a)$ or $t_{ij}(x_{ij})$, which is assumed to be a strictly increasing function with respect to the corresponding link flow. The travel time of GVs on path $k_g \in K_g^{rs}$ between the O–D pair $(r, s)$ is a function with respect to all the path flows, denoted by $c_{k_g}^{rs}(\mathbf{f})$ with the expression:

$$c_{k_g}^{rs}(\mathbf{f}) = \sum_{a\in A} t_a(x_a)\cdot\delta_{a,k_g}^{rs} \tag{21}$$

where the path flow $\mathbf{f} = (f_{k_g}^{rs} \geq 0, f_{k_e^m}^{rs} \geq 0 | r \in R, s \in S, m \in M, k_g \in K_g^{rs}, k_e^m \in K_{e,m}^{rs})^T$.

The dwell time function of BEVs at the battery swapping station $i \in I$ is assumed to be the same for each group $m \in M$, denoted by $d_i(y_i)$. It is further assumed that $d_i(y_i)$, $i \in I$ is a strictly increasing function with respect to the battery swapping flow of BEVs. The generalized travel time of the feasible BSAP $k_e^m \in K_{e,m}^{rs}$ for BEVs in group $m \in M$ includes three components - travel time on the path, dwell time taken at the swapping stations and the travel time converted from the battery swapping cost using the VOT - denoted by $c_{k_e^m}^{rs}(\mathbf{f})$ with the expression:

$$c_{k_e^m}^{rs}(\mathbf{f}) = \sum_{a\in A} t_a(x_a)\cdot\delta_{a,k_e^m}^{rs} + \sum_{i\in I} d_i(y_i)\delta_{i,k_e^m}^{rs} + \sum_{i\in I}\lambda_m\delta_{i,k_e^m}^{rs}/\tau \tag{22}$$

At the UE state, neither GV nor BEV driver can reduce his (generalized) travel time by unilaterally changing paths, namely the (generalized) travel time on all used paths is equal and no greater than that of non-used paths. For GVs, the travel time on all used paths for O–D pair $(r, s)$is equal to the minimum path travel time denoted by $\mu_g^{rs}$, while for BEVs in group $m \in M$, the generalized travel time on the used BSAPs equals the minimum travel time on all the feasible BSAPs denoted by $\mu_{e,m}^{rs}$. The UE conditions can be mathematically described by:

$$\text{If } f_{k_g}^{rs} = 0 \text{ then } c_{k_g}^{rs} - \mu_g^{rs} \geq 0, \forall r \in R, s \in S, k_g \in K_g^{rs} \tag{23}$$

$$\text{If } f_{k_g}^{rs} > 0 \text{ then } c_{k_g}^{rs} - \mu_g^{rs} = 0, \forall r \in R, s \in S, k_g \in K_g^{rs} \tag{24}$$

$$\text{If } f_{k_e^m}^{rs} = 0 \text{ then } c_{k_e^m}^{rs} - \mu_{e,m}^{rs} \geq 0, \forall r \in R, s \in S, m \in M, k_e^m \in K_{e,m}^{rs} \tag{25}$$

$$\text{If } f_{k_e^m}^{rs} > 0 \text{ then } c_{k_e^m}^{rs} - \mu_{e,m}^{rs} = 0, \ \forall r \in R, s \in S, m \in M, k_e^m \in K_{e,m}^{rs} \tag{26}$$

## 3. Convex programming model

Following the Beckmann's formulation for the conventional UE conditions, the UE conditions shown by Eqs. (23)–(26) can be formulated by the following strictly convex programming model with $\mathbf{x}=(x_a, a \in A)^T$and $\mathbf{y}=(y_i, i \in I)^T$:

**[*UE-BEV&GV*]**

$$\min_{\mathbf{x},\mathbf{y}} \quad \sum_{a\in A}\int_0^{x_a} t_a(x)dx + \sum_{i\in I}\int_0^{y_i} d_i(y)dy + \sum_{i\in I}\sum_{m\in M}(y_{i,m}\lambda_m/\tau) \tag{27}$$

subject to the constraints (13)–(20).

It can be readily demonstrated that the model [UE-BEV&GV] has a unique solution of link flow $\mathbf{x}$ and battery swapping flow $\mathbf{y}$ due to the strict convexity of link travel time functions and the dwell time functions. However, the uniqueness of link flow and swapping flow for each group of BEVs with different usable battery capacity cannot be guaranteed.

The model [UE-BEV&GV] is also applicable for the case with the nonhomogeneous initial electricity of BEVs by adding some dummy origins and links. To be specific, the BEVs with different initial amount of electricity in the same group are

further divided into different classes in term of their initial amount of electricity. In the same spirit of the technique proposed by Adler et al. (2016), we can first create a dummy origin and then add a dummy link from the dummy origin to the original origin on which the electricity consumption is exactly the difference between initial amount of electricity and the usable capacity for each class of BEVs. Moreover, based on definition of minimum comfortable remaining energy with which drivers are free from the range anxiety (Franke et al., 2012), the model [UE-BEV&GV] can be extended to incorporate the effect of driving range anxiety by using a new usable battery capacity $W'_m = W_m - W_m^{comf}$ where $W_m^{comf}$ is the minimum comfortable remaining energy for drivers of BEV.

It should be noted that the model [UE-BEV&GV] is distinct from the UE models proposed by Jiang et al. (Jiang and Xie, 2014; Jiang et al., 2014; Jiang et al., 2012) and He et al. (2014). Specifically, the model [UE-BEV&GV] is a generalization of the UE models developed by Jiang and his research collaborators (Jiang and Xie, 2014; Jiang et al., 2014; Jiang et al., 2012) where no swapping stations are considered. On the other hand, the models proposed by He et al. (2014) involves the choice of BEV drivers for the charging amount in addition to the choice for the route from their origin to destination. In this regard, the feasibility of their alternative paths not only depends on whether their battery is charged or not, but also is affected by the amount of electricity to be charged at a charging station. In a whole, for the model formulation and algorithm design, this study is distinct from that of He et al. (2014) in three aspects. First, He et al.'s models were formulated based on the original network where *usable path* was defined for BEV. Their usable path is indeed a physical path with one feasible charging pattern, i.e., the charging pattern with the minimum charging cost. Nevertheless, our UE model have to be formulated with resort to network representation where BSAP is defined for BEV. For each physical path in the original network, there may exist multiple usable BSAP, each corresponding to a battery swapping pattern. Second, the charging time at a charging stations in their models is a function with respect to the charging amount, which can be pre-determined for a given path. In contrast, the dwell time at a battery swapping station in our model is assumed to be a function with respect to the battery swapping flow, thus its value can only be known after the swapping flow at equilibrium state is obtained. Third, in each iteration of their algorithm, a new usable path was generated via a mixed integer linear programming. The computational efficiency is limited by the commercial solver for the mixed integer linear programming problem. In this study, however, the descent-direction based algorithmic scheme (such as the Frank–Wolfe algorithmic framework) where the descent direction is found by multi-label method in a pseudo-polynomial time, can be applied to solve our model readily. Details for our algorithm design will be discussed at length in the subsequent section.

## 4. Solution algorithm

The F–W algorithmic scheme is appropriate for solving the model [UE-BEV&GV] in view of its convexity and decomposable formulation structure. Finding a descent direction at each iteration is the core of any F–W algorithmic schemes. With regard to the model [UE-BEV&GV], the descent-direction finding problem at the $n$th iteration for a given path flow $\mathbf{f}^{(n)}$ can be formulated as the following linear programming model:

**[*LP-BEV&GV*]$^{(n)}$**:

$$\min_{\mathbf{h}_g^{(n)},\mathbf{h}_e^{(n)}} \quad z\left(\mathbf{h}_g^{(n)},\mathbf{h}_e^{(n)}\right) = \sum_{r\in R}\sum_{s\in S}\sum_{k_g\in K_g^{rs}} c_{k_g}^{rs}\left(\mathbf{f}^{(n)}\right)\cdot h_{k_g}^{rs(n)} + \sum_{r\in R}\sum_{s\in S}\sum_{m\in M}\sum_{k_e^m\in K_{e,m}^{rs}} c_{k_e^m}^{rs}\left(\mathbf{f}^{(n)}\right)\cdot h_{k_e^m}^{rs(n)} \tag{28}$$

subject to

$$\sum_{k_g\in K_g^{rs}} h_{k_g}^{rs(n)} = q_g^{rs},\ \forall r\in R, s\in S \tag{29}$$

$$\sum_{k_e^m\in K_{e,m}^{rs}} h_{k_e^m}^{rs(n)} = q_{e,m}^{rs},\ \forall r\in R, s\in S, m\in M \tag{30}$$

$$h_{k_g}^{rs(n)} \geq 0, h_{k_e^m}^{rs(n)} \geq 0\ ,\ \forall r\in R, s\in S, m\in M, k_g\in K_g^{rs}, k_e^m\in K_{e,m}^{rs} \tag{31}$$

where $h_{k_g}^{rs(n)}$ and $h_{k_e^m}^{rs(n)}$ denote the auxiliary path flows of GV and BEV in the group $m\in M$ respectively, which are grouped into two vectors: $\mathbf{h}_g^{(n)} = (h_{k_g}^{rs(n)},\ k_g\in K_g^{rs}, r\in R, s\in S)^T$ and $\mathbf{h}_e^{(n)} = (h_{k_e^m}^{rs(n)}, k_e^m\in K_{e,m}^{rs}, r\in R, s\in S, m\in M)^T$.

The linear programming model [LP-BEV&GV]$^{(n)}$ can be equivalently decomposed into $|M|+1$ (where $|M|$ is the cardinality of set $M$) separated linear programming models for GV and each group of BEV respectively:

**[*LP-GV*]$^{(n)}$**:

$$\min_{\mathbf{h}_g^{(n)}} \quad z_g\left(\mathbf{h}_g^{(n)}\right) = \sum_{r\in R}\sum_{s\in S}\sum_{k_g\in K_g^{rs}} c_{k_g}^{rs}\left(\mathbf{f}^{(n)}\right)\cdot h_{k_g}^{rs(n)} \tag{32}$$

subject to

$$\sum_{k_g\in K_g^{rs}} h_{k_g}^{rs(n)} = q_g^{rs},\ \forall r\in R, s\in S \tag{33}$$

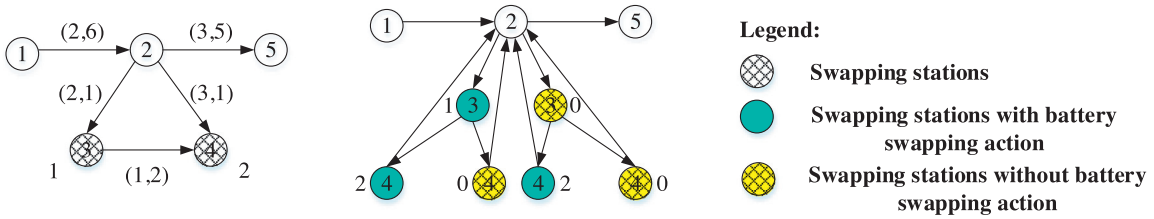


**(a) Original network** **(b) Network representation with battery swapping action based paths**

**Fig. 2.** Illustrative example I.

$$h_{k_g}^{rs(n)} \geq 0, \forall r \in R, s \in S, k_g \in K_g^{rs} \tag{34}$$

For each BEV group $m \in M$, we have
**[*LP-BEV$_m$*]$^{(n)}$**:

$$\min_{\mathbf{h}_{e,m}^{(n)}} \quad z_e\left(\mathbf{h}_{e,m}^{(n)}\right) = \sum_{r\in R}\sum_{s\in S}\sum_{k_e^m \in K_{e,m}^{rs}} c_{k_e^m}^{rs}\left(\mathbf{f}^{(n)}\right) \cdot h_{k_e^m}^{rs(n)} \tag{35}$$

subject to

$$\sum_{k_e^m \in K_{e,m}^{rs}} h_{k_e^m}^{rs(n)} = q_{e,m}^{rs}, \forall r \in R, s \in S \tag{36}$$

$$h_{k_e^m}^{rs(n)} \geq 0, \forall r \in R, s \in S, k_e^m \in K_{e,m}^{rs} \tag{37}$$

The linear programming model [LP-GV]$^{(n)}$ can be solved by the all-or-nothing traffic assignment method, i.e., assigning the traffic demand of GVs between each O–D pair to the shortest path between that O–D pair given the value of link travel time $t_a^{(n)} = t_a(x_a^{(n)}), a \in A$ where $x_a^{(n)}$ is the traffic flow on link $a$ at the $n$th iteration. Hence, the conventional shortest path algorithm like the Dijkstra's algorithm (Dijkstra, 1959), can be applied to solve the model [LP-GV]$^{(n)}$ efficiently. Similarly, the all-or-nothing traffic assignment method can be used to solve the linear programming model [LP-BEV$_m$]$^{(n)}$ provided that we can find the shortest BSAP for each O–D pair given the generalized travel time aggregating the link travel time $t_a^{(n)} = t_a(x_a^{(n)}), a \in A$, the dwell time $d_i^{(n)} = d_i(y_i^{(n)}), i \in I$ where $y_i^{(n)} = \sum_{m\in M} y_{i,m}^{(n)}$ and $y_{i,m}^{(n)} = \sum_{r\in R}\sum_{s\in S}\sum_{k_e^m \in K_{e,m}^{rs}} f_{k_e^m}^{rs(n)} \delta_{i,k_e^m}^{rs}$ and the travel time converted form the battery swapping cost $\lambda_m$. Therefore, finding the shortest BSAP is to solve the following problem:

$$\min_{k_e^m \in K_{e,m}^{rs}} c_{k_e^m}^{rs(n)} = \sum_{a\in A} t_a^{(n)} \cdot \delta_{a,k_e^m}^{rs} + \sum_{i\in I} d_i^{(n)} \delta_{i,k_e^m}^{rs} + \sum_{i\in I} \lambda_m \delta_{i,k_e^m}^{rs}/\tau \tag{38}$$

### *4.1. Multi-label method for solving the shortest battery swapping action based path problem:* $\min_{k_e^m \in K_{e,m}^{rs}} c_{k_e^m}^{rs(n)}$

The proposed shortest battery swapping action based path problem (SBSAPP) shown by Eq. (38) is different from the weight constrained shortest path problem (Laporte and Pascoal, 2011; Smith et al., 2012) because the state of charge (i.e., the level of electricity) of a BEV reaches its usable battery capacity again after each battery swapping action. It is also significantly distinct from the conventional shortest path problem of GV since the shortest BSAP may have loops due to the detours to swap the depleted battery for a fully charged one. In addition, the shortest BSAP may pass over a swapping station without a battery swapping action. In the network shown in Fig. 2(a), for example, each link is associated with two values in bracket, i.e., the travel time and electricity consumption on that link. Each swapping node is associated a value beside it in the figure, which denotes the sum of the dwell time and travel time converted form the battery swapping cost. Fig. 2(b) is the represented network with BSAPs. We assume that the usable battery capacity of BEV is 10 units and BEVs set out from node 1 with fully charged batteries. Therefore we can infer that the shortest path for GV is $1 \to 2 \to 5$, whereas the shortest BSAP for BEV is $1 \to 2 \to \hat{3} \to 4 \to 2 \to 5$ due to their limited driving range. It can be seen that the shortest BSAP of BEV have a loop, i.e., $2 \to \hat{3} \to 4 \to 2$, and the BEVs pass over node 4 without swapping a battery.

For a physical path $\xi_{xy}$ from node $x$ to node $y$ in the network $G=(N, A)$, let $\hat{\xi}_{xy}(l)$ denote a BSAP with $l$ battery swapping actions, generated from the physical path $\xi_{xy}$. Let $\hat{w}[\hat{\xi}_{xy}(l)]$ denote the electricity consumption of a BEV from its last battery swapping action along the BSAP until node $y$ if node $y$is the destination $s$ or there is no battery swapping action at node $y$. Otherwise, $\hat{w}[\hat{\xi}_{xy}(l)] = 0$, which implies that the battery of the BEV has not yet been consumed after swapping the battery

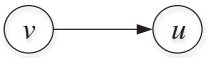


**Fig. 3.** Illustrative example II.

at the swapping station $y$. Assuming that the battery swapping sequence along the path $\hat{\xi}_{xy}(l)$ is coded by $\hat{v}_1, \hat{v}_2, \ldots, \hat{v}_{l-1}, \hat{v}_l$, where $\hat{v}_k \in I, k = 1, 2, \ldots, l$, we have

$$\hat{w}[\hat{\xi}_{xy}(l)] = \begin{cases} w[\xi_{xy}], \text{ if } l = 0 \\ w[\sigma_{\hat{\xi}_{xy}}(\hat{v}_l, y)], \text{ if } l > 0, (y = s) \text{ or } (y \neq s \text{ and } \hat{v}_l \neq y) \\ 0, \text{ if } l > 0, y \neq s \text{ and } \hat{v}_l = y \end{cases} \tag{39}$$

For the sake of presentation, $\hat{w}[\hat{\xi}_{xy}(l)]$ is referred to as the path auxiliary value of $\hat{\xi}_{xy}(l)$. It can be seen that $W_m - \hat{w}[\hat{\xi}_{xy}(l)]$ is the residual battery capacity of a BEV in the group $m \in M$ after the completion of its trip along the BSAP $\hat{\xi}_{xy}(l)$. However, the path auxiliary value $\hat{w}[\xi_{xy}(l)]$ may not be additive, namely:

$$\hat{w}[\hat{\xi}_{xy}(l)] \neq \hat{w}[\hat{\xi}_{xz}(l_1)] + \hat{w}[\hat{\xi}_{zy}(l_2)] \tag{40}$$

where $l_1, l_2 \geq 0$ and $l_1 + l_2 = l$; $\hat{\xi}_{xz}(l_1)$ from node $x$ to node $y$ and $\hat{\xi}_{zy}(l_1)$ from $z$ to $y$are two sub-paths for the path $\hat{\xi}_{xy}$ with $l_1$ and $l_2$ battery swapping actions, respectively.

The non-additivity of the path auxiliary value enables us to create multiple labels at each node for solving the SBSAPP from origin $r$ to destination $s$ by means of the label setting or label correcting methods. In other words, each node will have multiple labels to represent all the non-dominated feasible paths in terms of the generalized travel time and the path auxiliary value from origin $s$ to that node. More specifically, a particular label at node $v \in N$ is coded by $b_k(v) \triangleq [c_k, \hat{w}_k, \gamma_k, \varepsilon_k]$ where $c_k$ and $\hat{w}_k$ are the generalized travel time and path auxiliary value of path $k$ from origin $r$ to node $v$, respectively; $\gamma_k$ is a path index that precedes path $k$ in the path; $\varepsilon_k$ is the node index, namely, $\varepsilon_k = v$. Let us use the following example to intuitively illustrate the label updating process, where only two adjacent nodes in a transportation network are explicitly considered.

Suppose we have label $k$ at node $v$ as shown in Fig. 3, namely, $b_k(v) = [c_k, \hat{w}_k, \gamma_k, v]$ . Then a label denoted by $b_m(u)$ at node $u$ will be generated from label $k$ if node $u$ is not a swapping station, i.e., $b_m(u) = [c_k + t_{vu}, \hat{w}_k + w_{vu}, k, u]$. If, on the other hand, the node $u$ is a swapping station, then two labels$b_m(u) = [c_k + t_{vu}, \hat{w}_k + w_{vu}, k, u]$, $b_n(u) = [c_k + t_{vu} + \lambda_m, 0, k, u]$ can be created from label $k$, which represent the cases when a battery swapping action is not taken or taken at node $u$ respectively. Note that the two labels are associated with node $u$ (without and with battery swapping action) on two different BSAPs in the represented network. Once a new label is generated, the feasibility check and dominance test are performed successively. The former is to check whether $\hat{w}_k$ of this new label is less or equal to the usable battery capacity. If so, it implies that the generated intermediate path is feasible and this label will be reserved, and discarded otherwise. The dominance test helps to eliminate the undesired intermediate paths, which have no possibility to be extended to the final optimal path, at an early stage. After the processing of feasibility check and dominance test, only the non-dominated feasible paths are retained.

The algorithm solving MCPPR is proposed by Laporte and Pascoal (2011) to find the minimum cost path with relays in the telecommunication networks where all the nodes are relay nodes. In the context of BEV, only the battery swapping station can be viewed as the relay node. Therefore, a conditional statement is initiated to distinguish the battery swapping station with the other common nodes. In addition, since the effect of road grade on the electricity consumption is incorporated in the developed model, there may exist negative electricity consumption due to the energy saving from regenerative braking of BEV. The modification of some related value is thus made so that the positive electricity saving is acceptable and its value should not exceed the usable battery capacity (See line 11 in the pseudocode shown below). Moreover, to perform the dominance test, a matrix is constructed by Laporte and Pascoal (2011) to store the path index with the minimum generalized travel time for each possible path auxiliary value. Their algorithm is applicable for the network composed of links with integer electricity consumption. Considering the non-integer electricity consumption on each link for BEVs in the real applications, the proposed matrix cannot be used due to its fixed dimension. Instead, we define a singly-linked list for each node $j \in N$ as $L_j$ to store the path index. The $h^{th}$ Structure NODE along the singly-linked list $L_j$, denoted by $s_{jh}$, contains two values (path auxiliary value *pav* and currently optimal path label index *pli*) and one pointer $p$. For the sake of presentation, a Structure NODE with specific values is represented by $s_{jh}$(*pav, pli, p*), and the two values from a specific Structure NODE are denoted by $s_{jh}.pav$ and $s_{jh}.pli$ respectively. The multi-label method for solving the SBSAPP (ML-SBSAPP) is an improved algorithm for solving MCPPR by relaxing its integer assumption. The pseudocode of ML-SBSAPP from origin $r$ to destination $s$ for BEVs in the group $m \in M$ are presented below:

**Pseudocode of ML-SBSAPP**

```
Initialize L_j ← nil for all j ∈ N; nK ← 1; b_nK ← [0, W_m − W_m^0, −, r]; K ← {1}
While K ≠ ∅ Do
    k ← one element in K with the minimum value of c_k;
    If (ε_k = s) Then
        Break
    EndIf
    K − {k}; i ← ε_k
    For anyj ∈ N and (i, j) ∈ A Do
        w ← ŵ_k + w_ij
        If (w ≤ W_m) then
            w = max {w, 0}
            If (for all h, s_jh.pav ≠ w) then
                nK ← nK + 1; K ← K ∪ {nK}; L_j ← L_j ∪ s_jh(w, nK, p);
                b_nK ← [c_k + t_ij, w, k, j]
            Else If (∃h such that (s_jh.pav = w) and (c_k + t_ij < c_{s_jh}))
                    nK ← nK + 1; K ← K ∪ {nK}; s_jh.pli = nK;
                    b_nK ← [c_k + t_ij, w, k, j]
                EndIf
            EndIf
            If (j ∈ I) and (w ≠ 0) then
                If (for all h, s_jh.pav ≠ 0) then
                    nK ← nK + 1; K ← K ∪ {nK}; L_j ← L_j ∪ s_jh(0, nK, p);
                    b_nK ← [c_k + t_ij + t_j, 0, k, j]
                Else If (∃h such that (s_jh.pav = 0)and (c_k + t_ij + t_j < c_{s_jh}))
                        nK ← nK + 1; K ← K ∪ {nK}; s_jh.pli = nK;
                        b_nK ← [c_k + t_ij + t_j, 0, k, j]
                    EndIf
                EndIf
            EndIf
        EndIf
    EndFor
EndWhile
```

Following Laporte and Pascoal (2011), it can be seen that worst case time complexity of the ML-SBSAPP is by $(10^i W_m|A| + 10^i W_m|N|log(max\{10^i W_m, |N|\}))$ for BEVs in the group $m \in M$, where $|A|$and $|N|$is the cardinality of set $A$ and $N$, and $i$ represents the maximum decimal places among the value of electricity consumption on all links. In other words, the ML-SBSAPP is a pseudo-polynomial time algorithm.

### 4.2. F–W algorithm for solving model [UE-BEV&GV]

By applying Dijkstra's algorithm and ML-SBSAPP to solve shortest path problem of GV and BEV respectively, we get the auxiliary path flow $\mathbf{h}_g^{(n)}$ and $\mathbf{h}_e^{(n)}$. Once auxiliary path flow $\mathbf{h}_g^{(n)}$ and $\mathbf{h}_e^{(n)}$ are found, auxiliary link flow $\tilde{\mathbf{x}}^{(n)}$ and swapping flow $\tilde{\mathbf{y}}^{(n)}$,which define the descent directions as $(\tilde{\mathbf{x}}^{(n)} - \mathbf{x}^{(n)})$ and $(\tilde{\mathbf{y}}^{(n)} - \mathbf{y}^{(n)})$, can be calculated by using the incidence relationships, that is,

$$\tilde{x}_a^{(n)} = \sum_{r\in R}\sum_{s\in S}\sum_{k_g\in K_g^{rs}} h_{k_g}^{rs(n)}\delta_{a,k_g}^{rs} + \sum_{r\in R}\sum_{s\in S}\sum_{m\in M}\sum_{k_e^m\in K_{e,m}^{rs}} h_{k_e^m}^{rs(n)}\delta_{a,k_e^m}^{rs}, \forall a \in A \tag{41}$$

$$\tilde{y}_{i,m}^{(n)} = \sum_{r\in R}\sum_{s\in S}\sum_{k_e^m\in K_{e,m}^{rs}} h_{k_e^m}^{rs(n)}\delta_{i,k_e^m}^{rs}, \forall i \in I, m \in M \tag{42}$$

Having had the descent directions, any line search methods, e.g., bisection method can be applied to obtain the optimal step size to achieve the maximum drop of the objective function value. The relative gap which is based on the change in the traffic flows between the two successive iterations can be used as a convergence criterion for the F–W algorithm. For example, the algorithm can terminate if

$$\frac{\sqrt{\sum_{a\in A}(x_a^{(n+1)} - x_a^{(n)})^2 + \sum_{i\in I}\sum_{m\in M}(y_{i,m}^{(n+1)} - y_{i,m}^{(n)})^2}}{\sum_{a\in A} x_a^{(n)} + \sum_{i\in I}\sum_{m\in M} y_{i,m}^{(n)}} \le \kappa \tag{43}$$

where $\kappa$ is a predefined constant.

As stated above, the specific steps of F–W algorithm, when applied to solve model [UE-BEV&GV], can be summarized as follows:

**Step 0:** Initialization. Perform all-or-nothing assignment based on $t_a = t_a(0)$, $\forall a \in A$ and $d_i = d_i(0)$, $\forall i \in I$. This yields a set of flows $\{x_a^{(1)}, y_{i,m}^{(1)}\}$, $\forall a \in A$, $i \in I$, $m \in M$. Set counter $n$: $=1$.

**Step 1:** Update. Set $t_a^{(n)} = t_a(x_a^{(n)})$, $\forall a \in A$ and $d_i^{(n)} = d_i(y_i^{(n)})$, $\forall i \in I$.

**Step 2:** Descent-direction finding. Perform all-or-nothing assignment based on $\{t_a^{(n)}, d_i^{(n)}\}$,$\forall a \in A$, $i \in I$. This yields a set of auxiliary flows $\{\tilde{x}_a^{(n)}, \tilde{y}_{i,m}^{(n)}\}$, $\forall a \in A$, $i \in I$, $m \in M$.

**Step 3:** Line search. Find $\theta_n$ at $n$th iteration by solving

$$\min_{\theta_n \in [0,1]} \sum_{a \in A} \int_0^{x_a^{(n)} + \theta_n (\tilde{x}_a^{(n)} - x_a^{(n)})} t_a(x)\, dx + \sum_{i \in I} \int_0^{\sum_m [y_{i,m}^{(n)} + \theta_n (\tilde{y}_{i,m}^{(n)} - y_{i,m}^{(n)})]} d_i(y) dy + \sum_{i \in I} \sum_{m \in M} \{[y_{i,m}^{(n)} + \theta_n (\tilde{y}_{i,m}^{(n)} - y_{i,m}^{(n)})]\lambda_m / \tau\}$$

**Step 4:** Move. Set $x_a^{(n+1)} = x_a^{(n)} + \theta_n (\tilde{x}_a^{(n)} - x_a^{(n)})$, $\forall a \in A$ and $y_{i,m}^{(n+1)} = y_{i,m}^{(n)} + \theta_n (\tilde{y}_{i,m}^{(n)} - y_{i,m}^{(n)})$, $\forall i \in I$, $m \in M$.

**Step 5:** Convergence test. If a convergence criterion is not met, set $n$: $=n+1$ and go to step 1; otherwise, stop and the set of equilibrium flows is $\{x_a^{(n+1)}, y_{i,m}^{(n+1)}\}$, $\forall a \in A$, $i \in I$.

## 5. User equilibrium with flow and road grade dependent electricity consumption rate

The former analysis assumes that the amount of electricity consumed by a BEV depends on road (link) length and grade only and is independent of link travel time/ speed of the BEV. Once the length and grade of each link are given, therefore, the set of feasible BSAPs between an O–D pair for BEVs can be pre-determined, and the path-based formulation for the UE problem of the mixed BEVs and GVs is mathematically well defined. Nevertheless, it has been found that the electricity consumption rate of the BEV on a road (link) is a function of the travel speed or the flow-dependent link travel time (Bigazzi and Clifton, 2015; Liu et al., 2015). Hence, it is more realistic to assume that the electricity consumption rate of BEVs on link $a \in A$ is a function of its length, grade and traffic flow, denoted by $\hat{\varphi}(l_a, g_a, x_a)$. Under such assumption, the aforementioned path-based formulation is inapplicable anymore because the set of the feasible BSAPs for the BEV cannot be pre-determined. More to the point, the feasibility of each BSAP depends on link flow pattern and BEV swapping flow pattern $\{\mathbf{x}, \mathbf{y}\}$.

He et al. (2014) have made a first attempt to formulate the UE conditions with the flow-dependent electricity consumption rate for BEVs in a transportation network with charging stations. However, their UE conditions are incomplete in the sense that they are unable to describe the UE state in some circumstances. The details will be elaborated in the next subsection.

### 5.1. UE conditions proposed by He et al. (2014)

He et al. (2014) first defined a *charging-depleting path* as a usable path with the electricity consumption of a BEV reaching its usable battery capacity between two adjacent charging stations along that path. Conversely, the *non-charging-depleting path* is specified as a usable path with electricity consumption of a BEV strictly less than its usable battery capacity between any two adjacent charging stations along that path. For the sake of presentation, we define the *inter-charging sub-path* as the sub-path between two adjacent charging stations or between the origin/destination and the nearest charging stations. In addition, *the charging-depleting inter-charging sub-path* is defined as the inter-charging sub-path along which the electricity consumption reaches the usable battery capacity. Then it can be seen that the charging-depleting path is the usable path with at least one charging-depleting inter-charging sub-path along it, whereas the non-charging-depleting path is the usable path with no charging-depleting inter-charging sub-paths along it.

It can be inferred that the usable path defined by He et al. for the BEVs in a network with charging stations is essentially the same with one of the feasible BSAPs with the minimum swapping cost, if all the charging stations are replaced by swapping stations and swapping cost is given. In addition, their charging-depleting path is exactly the feasible BSAP with at least one inter-swapping sub-path along which the electricity consumption reaches the usable battery capacity. Moreover, the inter-charging sub-path can be viewed as the inter-swapping sub-path if charging stations are replaced by swapping stations. After defining these paths, they proceeded to propose the following UE conditions for the BEVs by taking into account the charging station constraints:

$$\text{If } f_{k_e}^{rs} > 0 \text{ then } w[\hat{\sigma}_{k_e}] \le W, \quad \forall r, s, k_e, \hat{\sigma}_{k_e} \tag{44}$$

$$\text{If } \left(f_{k_e}^{rs} > 0\right) \text{ and } \left(\exists \hat{\sigma}_{k_e} \text{ where } w[\hat{\sigma}_{k_e}] = W\right), \text{then } c_{k_e}^{rs} \le \pi^{rs}, \quad \forall r, s, k_e \tag{45}$$

$$\text{If } \left(f_{k_e}^{rs} > 0\right) \text{ and } \left(\forall \hat{\sigma}_{k_e}, w[\hat{\sigma}_{k_e}] < W\right), \text{then } c_{k_e}^{rs} = \pi^{rs}, \quad \forall r, s, k_e \tag{46}$$

$$\text{If} \left(f_{k_e}^{rs} = 0\right) \text{ and } \left(\forall \hat{\sigma}_{k_e}, w[\hat{\sigma}_{k_e}] \le W\right), \text{then } c_{k_e}^{rs} \ge \pi^{rs}, \quad \forall r, s, k_e \tag{47}$$

where $k_e$denotes any usable path for BEVs in a network with charging stations; $w[\hat{\sigma}_{k_e}]$ is the amount of electricity consumed by a BEV on the inter-charging sub-path $\hat{\sigma}_{k_e}$; $W$ is the usable battery capacity of the BEVs; $c_{k_e}^{rs}$ is the total travel time on path $k_e$ and $\pi^{rs}$ is the minimum travel time on all the non-charging-depleting paths.

As elaborated by He et al. (2014), condition (44) guarantees that all the utilized paths are usable since the electricity consumption of any inter-charging sub-path does not exceed the usable battery capacity. Conditions (45) and (46) jointly ensure that the travel time on all the utilized paths is no larger than or equal to $\pi^{rs}$ depending on whether they are

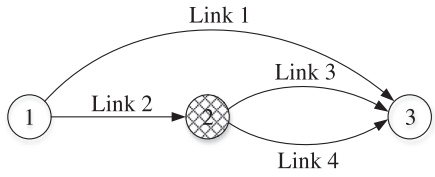


**Fig. 4.** Illustrative network example III (prismatic filled node denotes the charging station).

charging-depleting paths or not. In addition, Eq. (47) specifies that the travel time on all the unutilized usable paths is no less than $\pi^{rs}$.

However, the aforementioned UE conditions fail to identify an essential characteristic of the traffic flow at UE state, namely, the noncommutativity of path flows on different paths. On one hand, Eqs. (45) and (46) ensure that the path flow on a charging-depleting path will not change to a non-charging-depleting path because the travel time on the former is less than or equal to the latter. On the other hand, both equations are formulated in an attempt to guarantee that the path flow on the latter will not change to the former, otherwise the feasibility of former path is violated due to the existing charging-depleting inter-charging sub-path along it. Nevertheless, it is possible that the path flows on two different usable paths sharing ***the same*** charging-depleting inter-charging sub-path can be changed unilaterally to further reduce some drivers' travel time without violating the feasibility of both paths, unless the travel time on them are equal. Besides, Eq. (47) implies that the path flow on the utilized paths will not change to unutilized usable paths because the travel time on the latter is no less than the former, however, for an unutilized charging-depleting path, the travel time on it can be any value since it may be impossible for the path flows on all the other utilized paths to change to it without violating the feasibility of it.

We now use a small network example shown in Fig. 4 to show that the UE conditions (44)–(47) fail to describe the UE behavior. Assume that there is one O–D pair with the travel demand of 10 units from origin node 1 to destination 3. BEVs are assumed to set out with usable battery capacity of 10 units and the charging cost at charging station is set to be zero. The link travel time functions and electricity consumption for each link are given by

Link 1: $t_1(x_1) = 5 + x_1^2/25; w_1(x_1) = 7 + x_1/2;$
Link 2: $t_2(x_2) = 3 + x_2^2/25; w_2(x_2) = 5 + x_2;$
Link 3: $t_3(x_3) = x_3^2/25; w_3(x_3) = 2 + x_3/2;$
Link 4: $t_4(x_4) = 1 + x_4^2/25; w_4(x_4) = 3 + x_4.$

It can be easily checked that $\mathbf{x}^{UE} = [5, 5, 5, 0]^T$ is the UE link flow solution and the correspondent UE path flow and path cost are given by (index for origin and destination in this example is omitted for simplicity).

$$f_1^{UE} = 5; c_1^{UE} = 6; f_2^{UE} = 5; c_2^{UE} = 5; f_3^{UE} = 0; c_3^{UE} = 5 \tag{48}$$

where paths 1, 2, 3 are composed of link 1, link 2 and 3, link 2 and 4, respectively. The results obviously show that the minimum travel cost on all non-charging-depleting paths is 6, i.e., $\pi = c_1 = 6$, which is contrary to Eqs. (47) and (48) where $c_3 = 5 \geq \pi$. Therefore, Eqs. (44)–(47) are unable to describe the UE conditions for this example. Moreover, if the link flow solution is $\mathbf{x} = [5, 5, 4, 1]^T$ and the correspondent path flow and path cost are given by

$$f_1 = 5; c_1 = 6; f_2 = 4; c_2 = 4.64; f_3 = 1; c_3 = 5.04 \tag{49}$$

which meet the conditions (44)–(47), however, are not UE solutions because the drivers on path 3 can change to path 2 to reduce their travel time. Hence, Eqs. (44)–(47) are neither sufficient nor necessary UE conditions when electricity consumption rate of BEV is flow-dependent. We will give different UE conditions below in the context of mixed BEVs and GVs with battery swapping stations and road grade constraints.

### 5.2. Sufficient and necessary UE conditions

For each path $k_e^m$ for the BEVs in the group $m \in M$, given that $W_m^0 = W_m$, we define the *depleting inter-swapping sub-path* as the inter-swapping sub-path along which the amount of electricity consumed by the BEV equals the usable battery capacity. All the inter-swapping sub-paths for the path $k_e^m$ are grouped into a set denoted by$A_{k_e^m} = \{\hat{\sigma}_{k_e^m}\} := \{\sigma_{k_e^m}(r, \hat{v}_{i_1}), \sigma_{k_e^m}(\hat{v}_{i_h}, s), \sigma_{k_e^m}(\hat{v}_{i_j}, \hat{v}_{i_{j+1}}), j = 1, 2, \ldots, h-1\}$where $\hat{v}_{i_1}, \hat{v}_{i_2}, \ldots, \hat{v}_{i_h}$ is the sequence of battery swapping stations with swapping actions along the path $k_e^m$; $\hat{\sigma}_{k_e^m}$ denotes any inter-swapping sub-path along the path $k_e^m$. In addition, we define another set for all the depleting inter-swapping sub-paths along the path $k_e^m$, i.e., $B_{k_e^m} := \{\hat{\sigma}_{k_e^m} \in A_{k_e^m} | w[\hat{\sigma}_{k_e^m}] = W_m\}$. Note that if for any$\hat{\sigma}_{k_e^m} \in A_{k_e^m}$, we have $w[\hat{\sigma}_{k_e^m}] < W_m$ or $w[\hat{\sigma}_{k_e^m}] > W_m$, then it follows that $B_{k_e^m} = \emptyset$. For the sake of presentation, we denote two different paths as $k_{e,1}^m$ and $k_{e,2}^m$ respectively. Then the UE conditions are given by

$$\text{If } f_{k_g}^{rs} = 0 \text{ then } c_{k_g}^{rs} - \mu_g^{rs} \geq 0, \forall r \in R, s \in S, k_g \in K_g^{rs} \tag{50}$$

$$\text{If } f_{k_g}^{rs} > 0 \text{ then } c_{k_g}^{rs} - \mu_g^{rs} = 0, \forall r \in R, s \in S, k_g \in K_g^{rs} \tag{51}$$

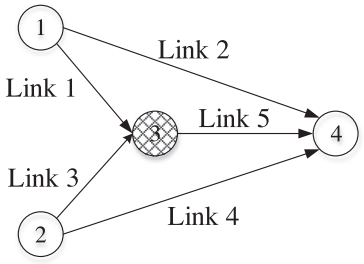


**Fig. 5.** Illustrative example IV (prismatic filled node denotes the battery swapping station).

$$If\ f^{rs}_{k^m_e} > 0, then\ w[\hat{\sigma}_{k^m_e}] \le W_m, \forall r, s, m, k^m_e, \hat{\sigma}_{k^m_e} \tag{52}$$

$$If\ \left(f^{rs}_{k^m_{e,1}} > 0\right)\&\left(f^{rs}_{k^m_{e,2}} > 0\right)\&\left(B_{k^m_{e,1}} = B_{k^m_{e,2}}\right), then\ c^{rs}_{k^m_{e,1}} = c^{rs}_{k^m_{e,2}},\ \forall r, s, m, k^m_{e,1}, k^m_{e,2} \tag{53}$$

$$If\ \left(f^{rs}_{k^m_{e,1}} > 0\right)\&\left(f^{rs}_{k^m_{e,2}} > 0\right)\&\left(B_{k^m_{e,1}} \supset B_{k^m_{e,2}}\right), then\ c^{rs}_{k^m_{e,1}} \le c^{rs}_{k^m_{e,2}},\ \forall r, s, m, k^m_{e,1}, k^m_{e,2} \tag{54}$$

$$If\ \left(f^{rs}_{k^m_{e,1}} > 0\right)\&\left(\left(f^{rs}_{k^m_{e,2}} = 0\right)\&\left(\forall \hat{\sigma}_{k^m_e}, w(\hat{\sigma}_{k^m_e}) \le W_m\right)\right)\&\left(B_{k^m_{e,1}} \supseteq B_{k^m_{e,2}}\right), then\ c^{rs}_{k^m_{e,1}} \le c^{rs}_{k^m_{e,2}},\quad \forall r, s, m, k^m_{e,1}, k^m_{e,2} \tag{55}$$

The following proposition reveals that under conditions (50)–(55), neither GV nor BEV driver can reduce his (generalized) travel time by unilaterally changing path, namely, the UE state has been obtained.

**Proposition.** Eqs. (50)–(55) are the sufficient and necessary UE conditions for the mixed BEVs and GVs.

**Proof.** It can be readily seen that the conditions (50)–(51) [i.e., Eqs. (23)–(24)] are the UE conditions for GVs since the behavior of GV drivers is not affected by the electricity consumption rate.

For BEVs, Eq. (52) are used to guarantee the feasibility of utilized path $k^m_e$. In addition, for any two distinct utilized feasible path $k^m_{e,1}$ and $k^m_{e,2}$ with positive path flows, i.e., $f^{rs}_{k^m_{e,1}} > 0$ and $f^{rs}_{k^m_{e,2}} > 0$, if $B_{k^m_{e,1}} = B_{k^m_{e,2}}$ holds which means that the drivers on both paths can be changed without violating the usable battery capacity constraint, then by defining that $c^{rs}_{k^m_{e,1}} = c^{rs}_{k^m_{e,2}}$ as Eq. (53), no drivers will change their paths because the travel time on both paths is equal. If, on the other hand, $f^{rs}_{k^m_{e,2}} > 0$ and $B_{k^m_{e,1}} \supset B_{k^m_{e,2}}$ as in Eq. (54) or $f^{rs}_{k^m_{e,2}} = 0$, $w(\hat{\sigma}_{k^m_{e,2}}) \le W_m$ for any $\hat{\sigma}_{k^m_{e,2}} \in A_{k^m_{e,2}}$ and $B_{k^m_{e,1}} \supseteq B_{k^m_{e,2}}$ as in Eq. (55) which mean that only the travel flow on the path $k^m_{e,1}$ can change to the path $k^m_{e,2}$ without violating the feasibility of that path, then by defining that $c^{rs}_{k^m_{e,1}} \le c^{rs}_{k^m_{e,2}}$ [see Eqs. (54)–(55)], no drivers on the path $k^m_{e,1}$ will change to the path $k^m_{e,2}$. It can be easily verified that the aforementioned analysis includes all the possible cases when BEV drivers will not change their paths although it is possible for them to do so without violating the usable battery capacity constraints. Hence Eqs. (52)–(55) are sufficient and necessary UE conditions for BEVs. □

Next, a small network is presented to illustrate that there may exist infinite numbers of UE link flow patterns for BEVs. Assume that there are two O–D pairs in the network shown in Fig. 5, i.e., (1, 4) and (2, 4), with the travel demand of 10 units for both O–D pairs. The BEV drivers set out from both origins with the usable battery capacity of 10 units and recharging/swapping cost at station is set to be zero. The link travel time and electricity consumption functions for each link are given by

Link 1: $t_1(x_1) = x_1^2/25$; $w_1(x_1) = 4 + x_1$;
Link 2: $t_2(x_2) = 3 + x_2^2/25$; $w_2(x_2) = 6 + x_2/3$;
Link 3: $t_3(x_3) = 1 + x_3^2/25$; $w_3(x_3) = 5 + x_3/2$;
Link 4: $t_4(x_4) = 4 + x_4^2/25$; $w_4(x_4) = 7 + x_4/4$;
Link 5: $t_5(x_5) = 1 + x_5^2/25$; $w_5(x_5) = 5 + x_5$.

We can see that there are two alternative paths for each O–D pair. The path 1 and path 2 for O–D pair (1, 4) can be represented by $1 \to 4$ and $1 \to 3 \to 4$, while for O–D pair (2, 4), the path 1 and path 2 are $2 \to 4$ and $2 \to 3 \to 4$. It can be easily checked that any path flow $f_2^{14} \in [0, 5]$ and the correspondent flows on the other paths $f_1^{14} = 10 - f_2^{14}$, $f_2^{24} = 5 - f_2^{14}$, $f_1^{24} = 5 + f_2^{14}$ are the UE path flow solution where the sub-path $3 \to 4$ is a depleting inter-swapping sub-path for path 2 of both O–D pairs. The corresponding UE link flow solutions are $x_1 = f_2^{14}, x_2 = 10 - f_2^{14}, x_3 = 5 - f_2^{14}, x_4 = 5 + f_2^{14}$, $x_5 = 5$ where $f_2^{14}$ can take any value between 0 and 5. It indicates that there exist infinite numbers of UE link flow solutions in the network shown in Fig. 5.

In light of non-uniqueness of UE state under flow-dependent electricity consumption the worst/best UE flow pattern with the maximum/minimum total (generalized) travel time might be defined to facilitate the design of robust policies (Lou et al., 2010). More explicitly, the worst UE flow pattern under flow-dependent electricity consumption can be found in theory by solving the following problem:

**[*W/B-UE-BEV&GV*]**

$$\max_{\mathbf{x},\mathbf{y}}/\min \quad \sum_{a\in A} t_a(x)x_a + \sum_{i\in I} d_i(y)y_i + \sum_{i\in I}\sum_{m\in M}(y_{i,m}\lambda_m/\tau) \tag{56}$$

subject to the constraints (13)–(20) and (50)–(55).

For the network in Fig. 5, [W/B-UE-BEV&GV] can be reduced to a one-dimensional constrained programming model. The worst and best UE flow patterns among the infinite number of UE solutions are given by $x_1=5$, $x_2=5$, $x_3=0$, $x_4=10$, $x_5=5$ and $x_1=2.5$, $x_2=7.5$, $x_3=2.5$, $x_4=7.5$, $x_5=5$ respectively.

Due to the complexity of UE conditions (50)–(55), it is still an open question whether they can be formulated as an optimization model or nonlinear complementarity model. Moreover, the infinite numbers of UE link flow solutions will essentially pose difficulty to predict the UE flow pattern when the electricity consumption rate is flow-dependent. Therefore, we leave this problem for our future study. For a small network as a numerical example in the next section, path enumeration is applied to obtain its UE solutions in order to further demonstrate the non-uniqueness of UE state when electricity consumption rate is assumed to be flow-dependent.

## 6. Numerical examples

In this section, two numerical examples are first presented to assess the proposed model and F–W algorithm with ML-SBSAPP for the UE problem with flow-independent electricity consumption rate. The algorithm is coded in C++ and run on a personal computer with Intel (R) Core (TM) Duo 3.4 GHz CPU. For simplicity, it is assumed that only one group of BEVs exists in the transportation networks and the market share of BEVs is same for all O–D pairs.

Assume that link travel time takes the form of Bureau of Public Roadside (BPR) function as following,

$$t_a(x_a) = t_a^0 \cdot \left[1 + 0.15 \times \left(\frac{x_a}{c_a}\right)^4\right], \forall a \in A \tag{57}$$

where $t_a^0$ denotes the free-flow travel time on link $a$, and $c_a$ represents the capacity of link $a$.

The dwell time at a battery swapping station is assumed in direct proportion to the average response time in an M/M/1 queue model (Kendall, 1953) in which number of arrivals per unit time equals swapping flow $y_i$ and service capacity rate of swapping station is $c_i$ (The condition that $y_i < c_i$ should be hold in M/M/1 queue model to ensure stability). By using Little's law (Little, 1961) and Taylor Series expansion, the closed-form expression for the average response time at the battery swapping station $i$ is given by

$$d_i(y_i) = \frac{1}{c_i - y_i} = \frac{\sum_{n=0}^{\infty}(y_i/c_i)^n}{c_i} \approx \frac{1}{c_i}\left(1 + \frac{y_i}{c_i} + \frac{y_i^2}{c_i^2}\right), \forall i \subseteq I \tag{58}$$

To ensure that free-flow dwell time (FFDT) equals a predefined value, we take the following form of dwell time function by multipling Eq. (58) with a constant, i.e.,

$$d_i(y_i) = (d_i^0 c_i)\left[\frac{1}{c_i}\left(1 + \frac{y_i}{c_i} + \frac{y_i^2}{c_i^2}\right)\right], \forall i \subseteq I \tag{59}$$

where $d_i^0$ denotes the FFDT at station $i$.

### 6.1. Nguyen–Dupius network

In order to validate the proposed model and algorithm, we first solve the model [UE-BEV&GV] in the Nguyen–Dupius network shown in Fig. 6. This small network consists of 13 nodes, 19 links and four O–D pairs. Free-flow travel time, capacity and electricity consumption of each link are tabulated in Table A.1. The total demand of BEVs and GVs for each O–D pairs is given by (Nguyen and Dupius, 1984)

$$q_{1\to 2} = 400veh/h; \quad q_{1\to 3} = 800veh/h;$$
$$q_{4\to 2} = 600veh/h; \quad q_{4\to 3} = 200veh/h.$$

There are two swapping stations in Nguyen–Dupius network, located at node 6 and 11. The FFDT at both stations are 2 min and capacity are 500 veh/h and 300 veh/h respectively.

Assume that market share of BEVs for all O–D pairs is 50%, the swapping cost is 60$ and VOT is 20 $/h. Moreover, the initial amount of electricity and usable battery capacity $W_m$ are supposed to be 24 kW h, which are consistent with the battery size of Nissan LEAF electric cars (Nissan, 2016). The equilibrium link flows and swapping flows are reported in Table A.3. It shows that solutions from F–W algorithm with ML-SBSAPP are consistent with optimal solutions of [UE-BEV&GV] by path enumeration (see Table A.2), which validates the effectiveness of proposed model and algorithm.

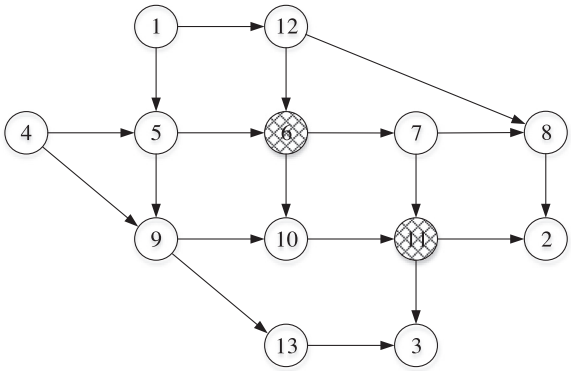


**Fig. 6.** Nguyen–Dupius network (prismatic filled node denotes the battery swapping station).

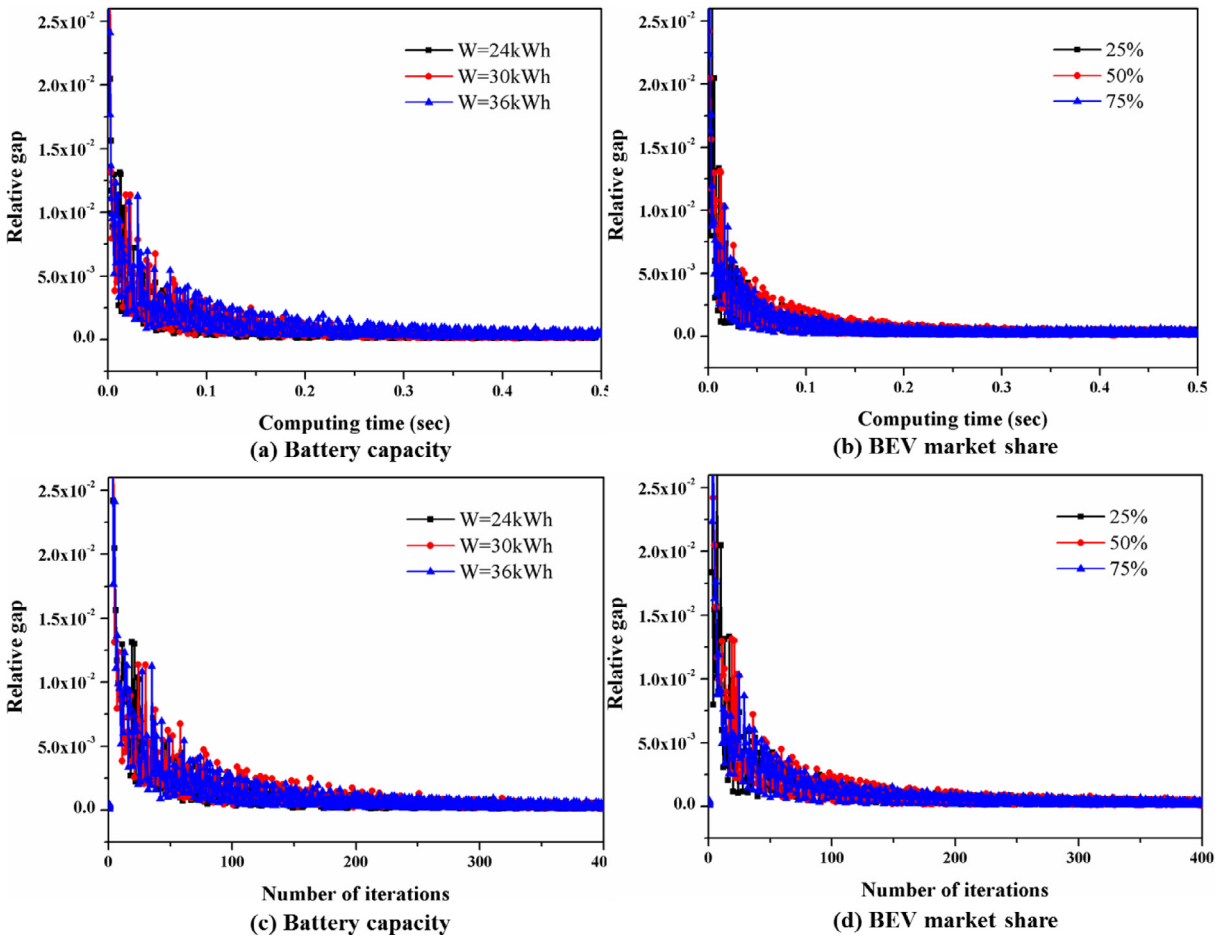


**Fig. 7.** Performance of proposed algorithm with different usable battery capacity and BEVs' market share in Nguyen–Dupius network.

To evaluate the impact of usable battery capacity on the convergence performance and computational time of F–W algorithm with ML-SBSAPP, another two usable battery capacity $W_m = 30$ kW h and $W_m = 36$ kW h are applied to the same network while BEVs' market share remains 50%. Similarly, to investigate the impact of BEVs' market share on the performance of algorithm, another two BEVs' market share with $W_m = 24$ kW h, namely, 25% and 75% are applied. Fig. 7 compares convergence performance and computational time of proposed algorithm with different usable battery capacity and BEVs' market share. Theoretically, the computational time of proposed algorithm may increase when usable battery capacity becomes larger because the worst case time complexity of ML-SBSAPP is an increasing function with respect to the usable battery capacity. However, Fig. 7 shows no much difference in the convergence pattern of algorithm given different usable

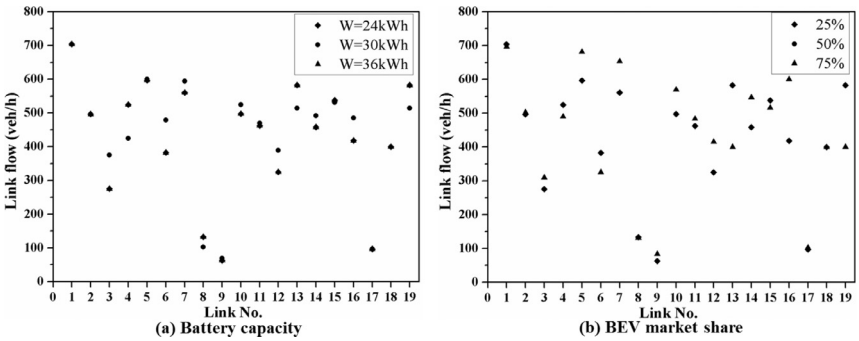


**Fig. 8.** Comparison of link flows with different usable battery capacity and BEVs' market share in Nguyen–Dupius network.

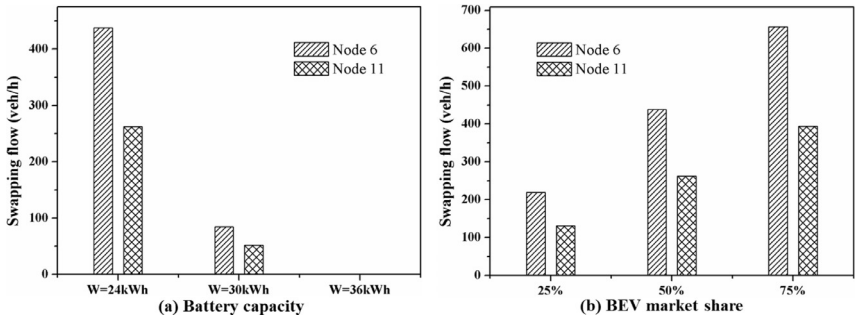


**Fig. 9.** Comparison of swapping flows with different usable battery capacity and BEVs' market share in Nguyen–Dupius network.

battery capacity and BEVs' market share. This discrepancy happens when the processing of algorithm in this specific example is far from the worst case of ML-SBSAPP, or the network is so small that the total computational time with different usable battery capacity is almost the same.

To investigate the link flow and swapping flow pattern given different usable battery capacity and BEV market share, the equilibrium link flows and swapping flows from six scenarios ($W_m = 24$ kW h, 30 kW h, 36 kW h and 25%, 50%, 75% BEVs' market share) are depicted in Figs. 8 and 9, respectively. Link flow variations with different usable battery capacity or BEVs' market share can be observed in Fig. 8, which reveals that both variations from usable battery capacity and BEVs' market share may have significant impact on the equilibrium flows of some links. As for swapping flows, it can be readily observed from Fig. 9 that swapping flows increase with smaller usable battery capacity and higher BEVs' market share. More likely, all the swapping flows will reduce to zero when usable battery capacity is increased to be 36 kW h. As expected, drivers of BEVs can finish their trips with less battery swapping activities when the usable battery capacity become larger.

### 6.2. Sioux-Falls network

To further test the impact of usable battery capacity, BEVs' market share on the convergence performance and computational time of F–W algorithm with ML-SBSAPP, [UE-BEV&GV] is then applied to the Sioux Falls network (see Fig. 10), which consists of 24 nodes, 76 links and 576 O–D pairs. The free-flow travel time, capacity of each link from He et al. (2014) and the O–D demands from Bar-Gera (2013) are used here. Electricity consumption of BEVs on each link are tabulated in Table A.4. Assume there are 4 swapping stations in the Sioux Falls network (see the prismatic filled nodes in Fig. 10). The FFDT and capacity of each station are tabulated in Table A.5. We first solve [UE-BEV&GV] with usable battery capacity $W_m = 24$ kW h, and the equilibrium link flows are reported in Table A.6. Then the aforementioned six scenarios are applied to Sioux Falls network. Fig. 11 depicts the convergence performance and computational time of F–W algorithm with different usable battery capacity and BEVs' market share. It can be seen that the algorithm converges to the equilibrium state within two minutes, which illustrate the potential application of proposed F–W algorithm with ML-SBSAPP in networks of large size. Furthermore, it can be observed that the computational time of proposed algorithm increases when usable battery capacity becomes larger and remains the same when BEVs' market share increases, which is consistent with the assertion that the worst case complexity of proposed algorithm is an increasing function with respect to the usable battery capacity and have nothing to do with BEVs' market share.

To further investigate the swapping flow pattern given different usable battery capacity and BEVs' market share, the equilibrium swapping flows under aforementioned six scenarios are depicted in Fig. 12. We can see that all the swapping flows will reduce to zero when usable battery capacity is increased to be 36 kWh. However, it does not necessarily mean that the swapping flows at all stations will decrease when usable battery capacity is increased from 24 kWh to 30 kWh, operators of

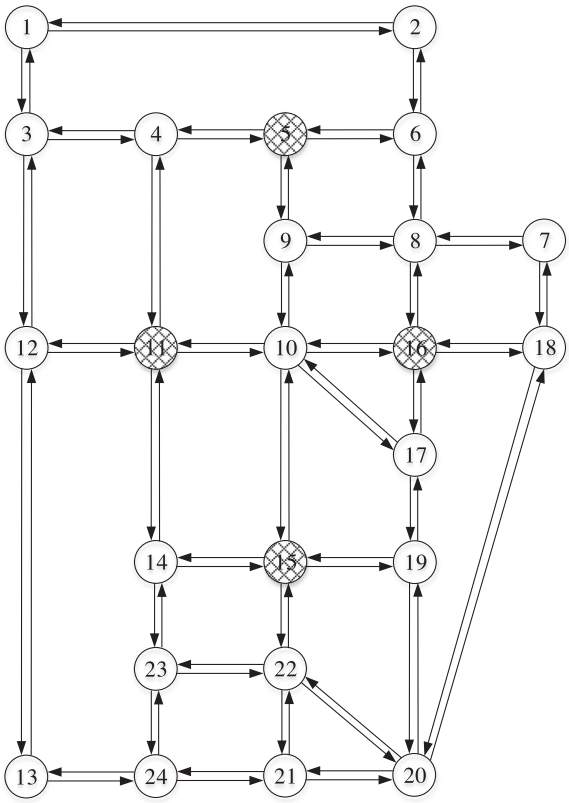


**Fig. 10.** Sioux Falls network (prismatic filled nodes denote swapping stations).

swapping stations therefore should adjust inventory of batteries in time to meet the demand at each station. Additionally, it can be readily seen from Fig. 12 that swapping flows at all stations increases as market share of BEV increases, so operators of swapping stations should increase the inventory of batteries in prospect of large-scale BEVs' uptake. However, the increasing ratio of swapping flows may not the same with that of BEVs' market share, which implies that the appropriate number of batteries in inventory should be recalculated each time the market share of BEV changes.

In addition to the usable battery capacity and BEVs' market share, we also explore the impact of some attributes of battery swapping stations, e.g., their capacity, FFDT, the number and deployment of swapping stations, on the algorithm performance as well as the swapping flow pattern. Specifically, three scenarios including the original capacity/FFDT, two times of the original capacity/FFDT and three times of the original capacity/FFDT are tested to gauge the impact of capacity/FFDT of battery swapping stations. As for the number and deployment of swapping stations, the details of scenarios can be found in Tables A.7 and A.8 respectively.

Fig. 13 depicts the convergence performance and computational time of F–W algorithm under different scenarios with respect to the capacity, FFDT, number and deployment of swapping stations. It can be seen that the algorithm converges to the equilibrium state within two minutes and the computational time of proposed algorithm slightly increases when the number of swapping stations becomes larger and remains the same when the other attributes of swapping stations change. This is because with more swapping stations, more labels would be generated in each node and propagated along the path, resulting in more times the link to be scanned and more comparisons to be made between labels.

As for their impact on the swapping flow pattern, the equilibrium swapping flows under aforementioned scenarios are depicted in Fig. 14. It seems that the increased station capacity and the decreased FFDT have led to the marginal increment of swapping flow in node 5 and the slight decrease of swapping flows in node 11, 15 and 16. However, the variations of swapping flows with respect to the change of station capacity and FFDT are not obvious. Fig. 14(c) suggests that the double-increase of number of swapping stations almost has nothing to do with the total demand for battery swapping and the newly-built swapping stations would attract the swapping flows in existing swapping stations to some degree. Nevertheless, this may not be true for the deployment of swapping stations since the Deployment 3 have led to nearly 5% more total swapping flows than Deployment 1 or 2 as revealed by Fig. 14(d). In addition, it shows that the distribution of swapping flows across different stations is also affected by the deployment of swapping stations. The appropriate number and deployment of swapping stations should thus be determined to regulate the total demand and distribution of swapping demand in a desired way.

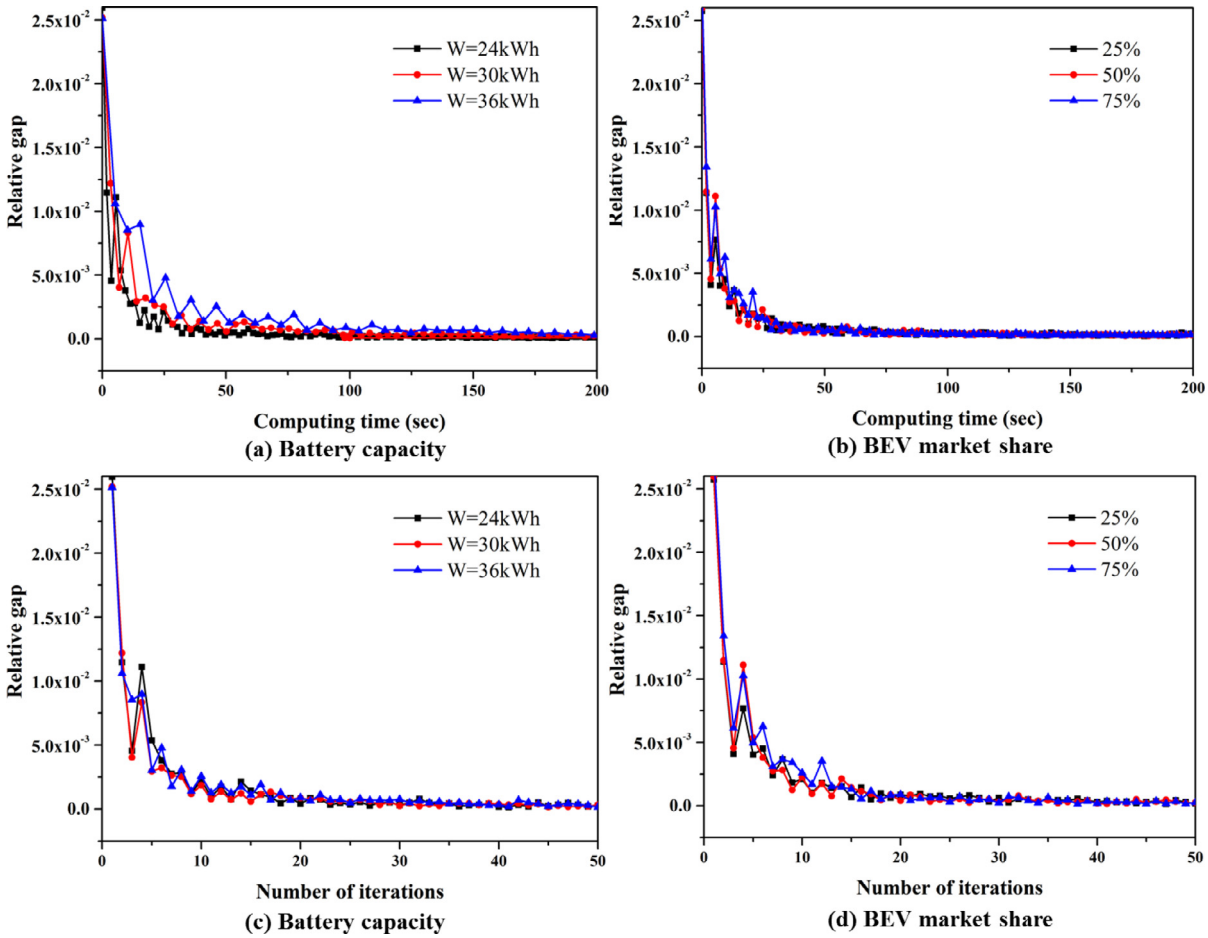


**Fig. 11.** Performance of proposed algorithm with different usable battery capacity and BEVs' market share in Sioux Falls network.

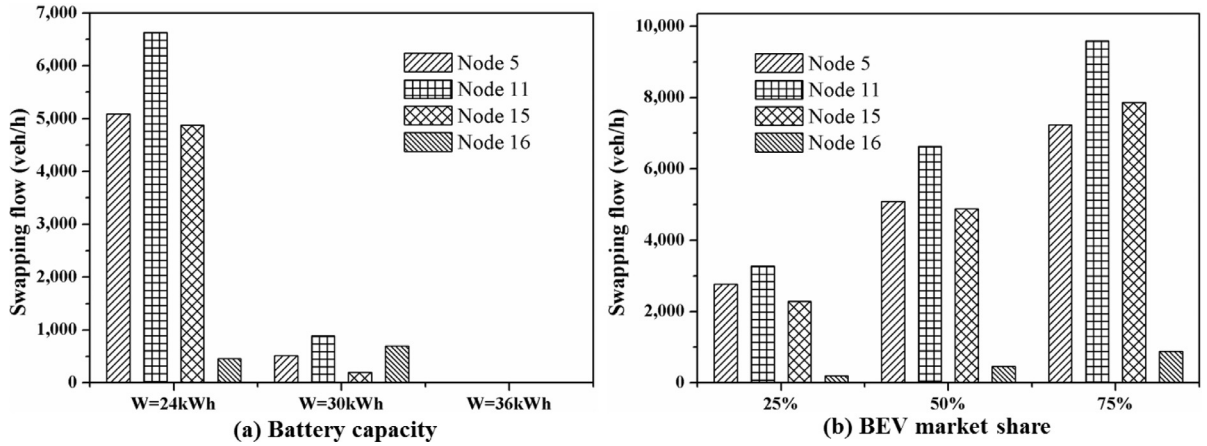


**Fig. 12.** Comparison of swapping flows with different usable battery capacity and BEVs' market share in Sioux Falls network.

### 6.3. Yang-Bell network

We next solve the UE problem with flow-dependent electricity consumption rate by path enumeration in a simple network designed by Yang and Bell (1997) to illustrate the non-uniqueness of its UE link flow solution (see Fig. 15). This small network consists of 7 nodes, 11 links and four O–D pairs. Free-flow travel time, capacity and free-flow electricity consumption of each link are tabulated in Table A.9. Market share of BEVs for all O–D pairs is assumed to be 50%, and the total O–D

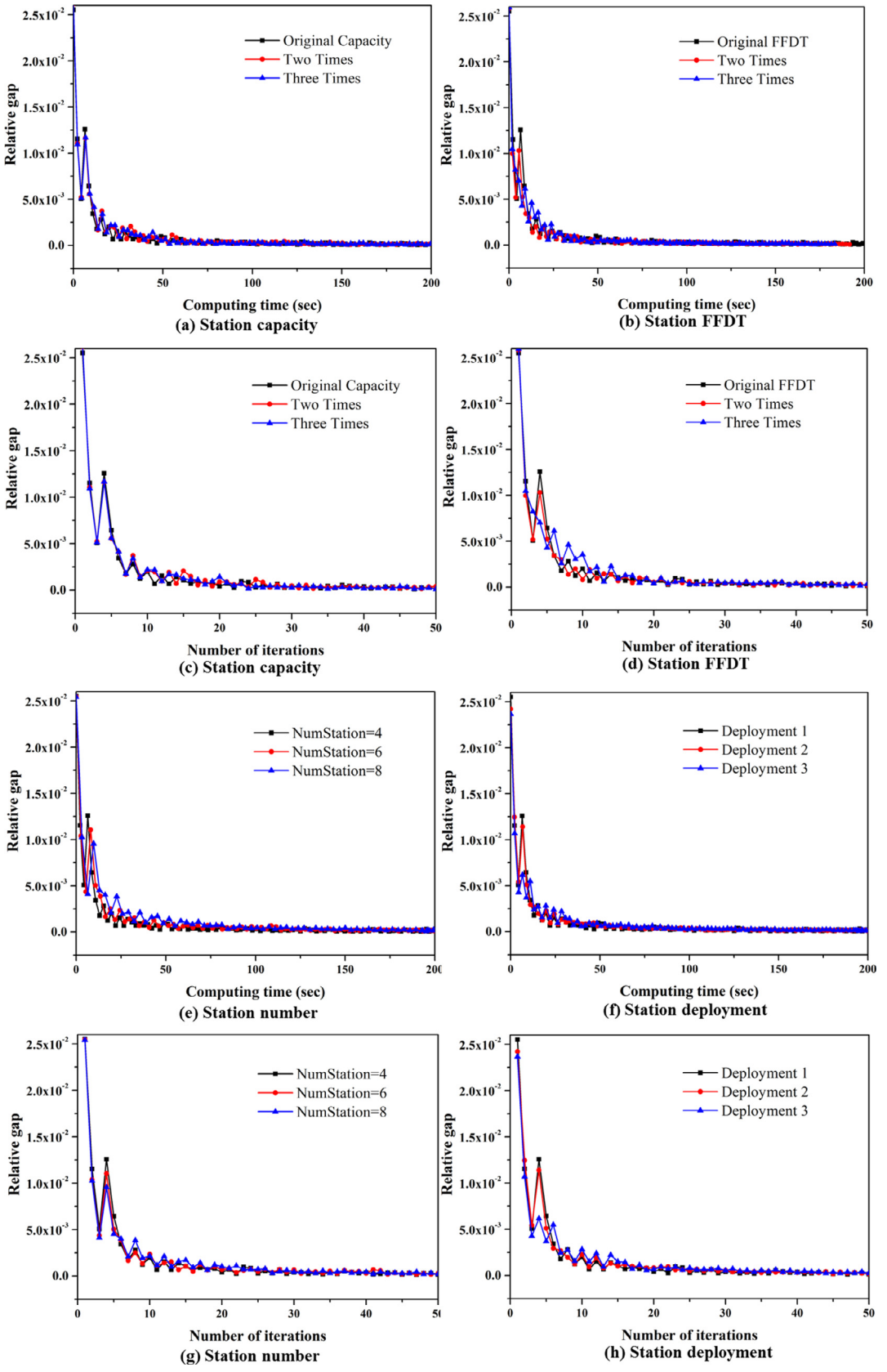


**Fig. 13.** Performance of proposed algorithm with different capacity, FFDT, number and deployment of swapping stations in Sioux Falls network.

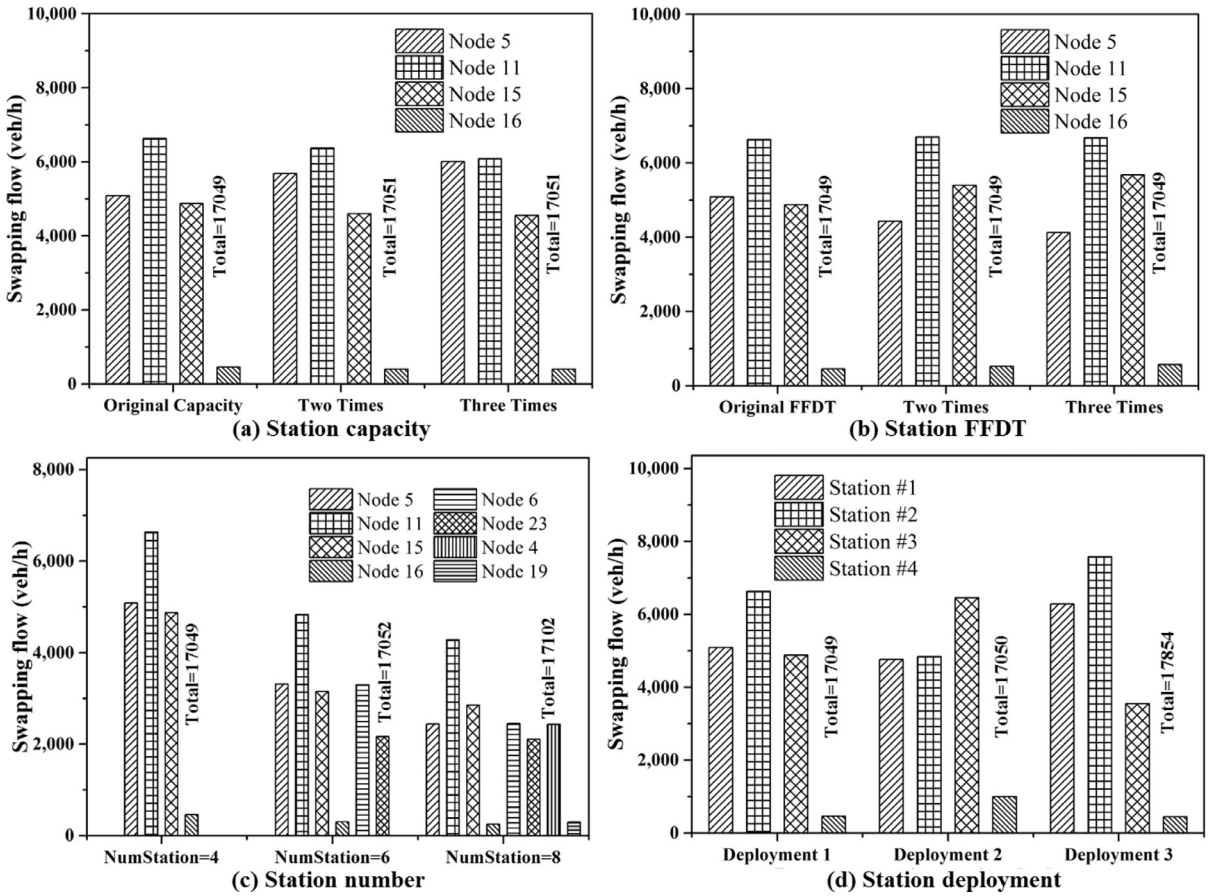


**Fig. 14.** Comparison of swapping flows with different capacity, FFDT, number and deployment of swapping stations in Sioux Falls network.

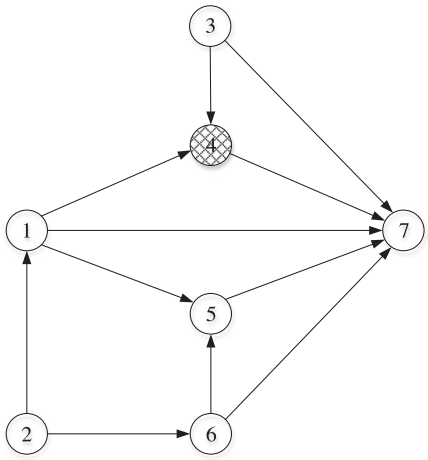


**Fig. 15.** The Yang–Bell network (prismatic filled nodes denote swapping stations).

demands of BEVs and GVs are given by

$$q_{1\to 7} = 600veh/h; \quad q_{2\to 7} = 500veh/h;$$
$$q_{3\to 7} = 500veh/h; \quad q_{6\to 7} = 400veh/h.$$

Given the fixed link length and grade, it is be assumed that flow-dependent electricity consumption takes the following form without loss of generality.

$$w_a(x_a) = w_a^0 \cdot (1 + 0.01x_a), \forall a \in A \tag{60}$$

where $w_a^0$ is the free-flow electricity consumption of link $a$, which is a function of link length and grade.

There is one swapping station in this simple network, located at node 4. For simplicity, dwell time and swapping cost at swapping stations for BEVs are set to be zero. Under the aforementioned conditions, there may exist many equilibrium solutions corresponding to its UE conditions and two of them are tabulated in Tables A.10–A.12 for illustration. It can be seen that both link flows and path flows are substantially different in the two equilibria, which poses a challenge to predict equilibrium flow pattern of BEVs and GVs in a network with battery swapping stations if the electricity consumption rate is flow-dependent.

## 7. Conclusions and future research

In this paper, the UE problem of the mixed BEVs and GVs in the transportation networks with battery swapping stations and road grade constraints has been investigated. Under the assumption that electricity consumption rate of the BEV is not affected by traffic flows, we formulate a nonlinear minimization model by incorporating effects of road grade on the electricity consumption rate and dwell time at battery swapping stations. The battery swapping action based paths are defined for BEVs in the represented network to facilitate the model building with flow-dependent dwell time at the battery swapping stations. The equivalence of the optimal solutions for the proposed model to UE conditions has been justified. F–W algorithmic framework is proposed to solve the model, where the shortest battery swapping action based path problem is involved in the descent-direction finding step. The descent direction is found by multi-label method in a pseudo-polynomial time. In addition, we relax the aforementioned assumption by assuming that the electricity consumption rate of BEVs is flow-dependent, and a system of inequalities are formulated to represent the UE conditions.

Two numerical examples are presented to illustrate the proposed nonlinear minimization model and algorithm, as well as to analyze the impact of usable battery capacity, BEVs' market share and some attributes of battery swapping stations on the equilibrium link flows and/or swapping flows. The results show that computational time of proposed algorithm increases when usable battery capacity or number of swapping stations become larger and swapping flows tend to increase with smaller usable battery capacity and higher BEVs' market share. Both the total swapping demand and distribution of swapping flows across different stations vary with the deployment of swapping stations, whereas they seem not affected by station capacity and FFDT, and the number of swapping stations only affects the distribution of swapping flows. Operators of swapping stations, therefore, should adjust the inventory of batteries each time usable battery capacity or BEVs' market share changes and the appropriate number and deployment of swapping stations can be determined to regulate the total demand and distribution of swapping demand in a desired way. Moreover, the system of inequalities for the UE problem with flow-dependent electricity consumption rate is solved in a small network by path enumeration to demonstrate the non-uniqueness of UE solutions. Our study serves as a useful guide for transportation planners and operators of battery swapping stations.

Further research work will be undertaken in several aspects. First of all, as mentioned in Section 5.2, it remains an open question whether and how the UE conditions with flow-dependent electricity consumption rate can be formulated as an optimization problem or nonlinear complementarity problem, as well as the algorithm to solve it. Second, the proposed UE model assumes that drivers of GVs are indifferent to flow-dependent fuel expense when they choose paths. Such assumption can be relaxed in future study and varitional inequality formulation will be used because drivers of BEVs and GVs may face different generalized link travel time functions. Finally, this study serves as a good reference for future extensions like the SUE or BRUE and it is also interesting to consider path reliability and several stochastic factors in the context of UE problem dedicated for BEVs, for example, range anxiety, drivers' familiarity with swapping stations, etc. With those stochastic factors, behavior of BEV drivers can be better described.

## Acknowledgements

We are indebted to two anonymous reviewers for their thoughtful comments and suggestions that have helped substantially improve this work. This study was partly supported by the research project "Studying Autonomous Vehicles Policies with Urban Planning of Toa Payoh in Singapore" funded by L2NIC of Singapore. The last author would also like to acknowledge support funding from National Natural Science Foundation of China (Grant No. 51378091) and Fundamental Research Funds for the Central Universities of China (Grants No. DUT12ZD203).

## Appendix. –Abbreviaitons, Notations and Tables

*Abbreviaitons*

| | |
|---|---|
| WCSPP | Weight constrained shortest path problem |
| FW-WCSPP | Frank–Wolfe method with the label-setting method solving the WCSPP |
| FW-MLS | Frank–Wolfe algorithmic framework with a modified one-to-all label-setting method |

| | |
|---|---|
| PG-PLS | Projected gradient method with a combined pre-processing and label-setting method |
| PLM-PLS | Partial linearization method with a combined pre-processing and label-setting method |
| CONOPT/PATH-CPLEX 12.2 | Iteration algorithms solved by CONOPT (or PATH) and CPLEX 12.2 |
| BSAP | Battery swapping action based path |
| SBSAPP | Shortest battery swapping action based path problem |
| MCPPR | Minimum cost path problem with relays |
| ML-SBSAPP | Multi-label method for solving the shortest battery swapping action based path problem |

*Notations*

| | |
|---|---|
| $N$ | Set of nodes |
| $A$ | Set of links, $A=\{a\}$ or $A=\{(i, j)\}$, $\forall i, j \in N$ |
| $R$ | Set of origins, $R=\{r\}$ |
| $S$ | Set of destinations, $S=\{s\}$ |
| $l_a$ | Length of link $a$ |
| $g_a$ | Road grade of link $a$ |
| $I$ | Set of battery swapping stations |
| $M$ | Set of BEVs groups in term of useable battery capacity, $M=\{m\}$ |
| $\|M\|$ | Cardinality of set $M$ |
| $W_m$ | Useable battery capacity of BEVs in group $m$ |
| $\lambda_m$ | Battery swapping cost for BEVs in the group $m$ |
| $W_m^0$ | Initial amount of electricity in the battery of BEVs in group $m$ |
| $\tau$ | Value of time for GVs and BEVs |
| $q_{e,m}^{rs}$ | Travel demands of BEVs in group $m \in M$ between O–D pair $(r, s)$ |
| $q_g^{rs}$ | Travel demands of GVs between O–D pair $(r, s)$ |
| $x_{ae}$ | BEV flow on link $a$ |
| $x_{ag}$ | GV flow on link $a$ |
| $x_a$ | Aggregated traffic flow on link $a$ |
| $y_i$ | Aggregated BEV battery swapping flow at the battery swapping station $i \in I$ |
| $y_{i,\,m}$ | Battery swapping traffic flow of BEVs in group $m$ at the battery swapping station $i \in I$ |
| $w_a$ | Amount of electricity consumed by a BEV traveling on link $a$ |
| $\phi(l_a, g_a)$ | Flow-independent electricity consumption function on link $a$ with respect to length $l_a$ and grade $g_a$ |
| $K_g^{rs}$ | Set of all the physical paths from an origin $r$ to a destination $s$for GVs |
| $w[p]$ | Amount of electricity consumed by a BEV traveling on path $p$ |
| $\sigma_p(v_i, v_j)$ | Sub-path of path $p$from nodes $v_i$ to $v_j$ |
| $K_{e,m}^{rs}$ | Feasible battery swapping action based paths for BEVs in group $m$ from origin $r$ to destination $s$ |
| $\oplus$ | Concatenation of two sub-paths |
| $f_{k_g}^{rs}$ | Traffic flow of GVs on path $k_g \in K_g^{rs}$between O–D pair $(r, s)$ |
| $f_{k_e^m}^{rs}$ | Traffic flow of BEVs in group $m$on the feasible battery swapping action based path $k_e^m \in K_{e,m}^{rs}$ between O–D pair $(r, s)$ |
| $\delta_{a,k_g}^{rs}$ | Path-link incidence indicator for GVs, which equals to 1 if path $k_g$ traverses link $a$ and 0 otherwise |
| $\delta_{a,k_e^m}^{rs}$ | Battery swapping action based path-link incidence indicator for BEVs in group $m$, which equals to 1 if the feasible battery swapping action based path $k_e^m$ traverses link $a$ and 0 otherwise |
| $\delta_{i,k_e^m}^{w}$ | Battery swapping action based path-swapping action incidence indicator which equals to 1 if the feasible battery swapping action based path $k_e^m$ traverses the swapping station $i \in I$where a battery swapping action is taken and 0 otherwise. |
| $t_a$ or $t_{ij}$ | Travel time function of link $a=(i, j)$, where $t_a(x_a)$ or $t_{ij}(x_{ij})$is a strictly increasing function with respect to the corresponding link flow $x_a$ or $x_{ij}$ |
| $c_{k_g}^{rs}$ | Travel time of GVs on path $k_g$ between O–D pair $(r, s)$, where $c_{k_g}^{rs}(\mathbf{f}) = \sum_{a\in A} t_a(x_a) \cdot \delta_{a,k_g}^{rs}$ is a function of all the path flows $\mathbf{f} = (f_{k_g}^{rs} \geq 0,\, f_{k_e^m}^{rs} \geq 0 \mid r \in R, s \in S, m \in M, k_g \in K_g^{rs}, k_e^m \in K_{e,m}^{rs})^T$ |
| $d_i$ | Dwell time function of BEVs in group $m$ at the battery swapping stations $i \in I$, where $d_i(y_i)$ is a strictly increasing function with respect to the battery swapping flow of BEVs $y_i$ |
| $c_{k_e^m}^{rs}$ | Generalized travel time of the feasible battery swapping action based path $k_e^m \in K_{e,m}^{rs}$ for BEVs in group $m$, where $c_{k_e^m}^{rs}(\mathbf{f}) = \sum_{a\in A} t_a(x_a) \cdot \delta_{a,k_e^m}^{rs} + \sum_{i\in I} d_i(y_i)\delta_{i,k_e^m}^{rs} + \sum_{i\in I} \lambda_m \delta_{i,k_e^m}^{rs}/\tau$ |
| $\mu_g^{rs}$ | Minimum path travel time for GVs between O–D pair $(r, s)$ |
| $\mu_{e,m}^{rs}$ | Minimum feasible battery swapping action based path travel time for BEVs in group $m$ between O–D pair $(r, s)$ |
| $\mathbf{x}$ | Vector of link flows, $\mathbf{x}=(x_a,\, a \in A)^T$ |
| $\mathbf{y}$ | Vector of battery swapping flows, $\mathbf{y}=(y_i,\, i \in I)^T$ |
| $W_m^{comf}$ | Minimum comfortable remaining energy that drivers of BEVs may suffer |

$\mathbf{f}^{(n)}$ Vector of path flow at the nth iteration of Frank–Wolfe algorithmic scheme

$h_{k_g}^{rs(n)}$ Auxiliary path flows of GVs at the nth iteration of Frank–Wolfe algorithmic scheme

$h_{k_e^m}^{rs(n)}$ Auxiliary path flows of BEVs in group $m$ at the nth iteration of Frank–Wolfe algorithmic scheme

$\mathbf{h}_g^{(n)}$ Vector of auxiliary path flows of GVs at the nth iteration of Frank–Wolfe algorithmic scheme, $\mathbf{h}_g^{(n)} = (h_{k_g}^{rs(n)},\ \forall k_g \in K_g^{rs}, r \in R, s \in S)^T$

$\mathbf{h}_e^{(n)}$ Vector of auxiliary path flows of BEVs in group $m$ at the nth iteration of Frank–Wolfe algorithmic scheme, $\mathbf{h}_e^n = (h_{k_e^m}^{rs(n)}, \forall k_e^m \in K_{e,m}^{rs}, r \in R, s \in S, m \in M)^T$

$x_a^{(n)}$ Aggregated traffic flow on link $a$ at the nth iteration of Frank–Wolfe algorithmic scheme

$t_a^{(n)}$ Travel time on link $a$ at the nth iteration of Frank–Wolfe algorithmic scheme

$d_i^{(n)}$ Dwell time of BEVs in group $m$ at the battery swapping stations $i \in I$ at the nth iteration of Frank–Wolfe algorithmic scheme

$c_{k_e^m}^{rs(n)}$ Generalized travel time of the feasible battery swapping action based path $k_e^m \in K_{e,m}^{rs}$ for BEVs in group $m$ at the nth iteration of Frank–Wolfe algorithmic scheme

$\xi_{xy}$ Physical path $\xi_{xy}$ from node $x$ to node $y$

$\hat{\xi}_{xy}(l)$ Battery swapping action based path with $l$ battery swapping actions, generated from the physical path $\xi_{xy}$

$\hat{w}[\hat{\xi}_{xy}(l)]$ Path auxiliary value of the battery swapping action based path $\hat{\xi}_{xy}(l)$.

$b_k(v)$ Label $k$ at the node $v \in N$, $b_k(v) \triangleq [c_k, \hat{w}_k, \gamma_k, v]$, where $c_k$ and $\hat{w}_k$ are the generalized travel time and auxiliary value of path $k$ from node $s$ to node $v$, respectively; $\gamma_k$is a path index that precedes path $k$ in the path.

$L_j$ Singly-linked list for node $j \in N$

$s_{jh}(pav, pli, p)$ The $h^{th}$ Structure NODE along the singly-lined list $L_j$, contains two values (path auxiliary value $pav$ and currently optimal path label index $pli$) and one pointer $p$

$\tilde{\mathbf{x}}^{(n)}$ Vector of auxiliary link flow at the $n^{th}$ iteration of Frank–Wolfe algorithmic scheme

$\tilde{\mathbf{y}}^{(n)}$ Vector of auxiliary battery swapping flow at the $n^{th}$ iteration of Frank–Wolfe algorithmic scheme,

$\kappa$ Predefined criterion (constant) for relative gap to terminate Frank–Wolfe algorithmic scheme

$\theta_n$ Step size at the nth iteration of Frank–Wolfe algorithmic scheme,

$\hat{\varphi}(l_a, g_a, x_a)$ Flow-dependent electricity consumption function on link $a$ with respect to length $l_a$, grade $g_a$ and link flow $x_a$

$k_e$ Usable path for BEVs in a network with charging stations

$\hat{\sigma}_{k_e}$ Inter-charging sub-path for usable path $k_e$

$W$ Usable battery capacity of BEVs in a network with charging stations

$c_{k_e}^{rs}$ Total travel time on path $k_e$

$\pi^{rs}$ Minimum travel time on all the non-charging-depleting paths

$f_{k_e}^{rs}$ Traffic flow of BEVs on path $k_e$ between O–D pair $(r, s)$

$\hat{\sigma}_{k_e^m}$ Inter-swapping sub-path along battery swapping action based path $k_e^m \in K_{e,m}^{rs}$ for BEVs in group $m$

$A_{k_e^m}$ Set of all the inter-swapping sub-paths along path $k_e^m$ for BEVs in group $m$ between O–D pair $(r, s)$, $A_{k_e^m} = \{\hat{\sigma}_{k_e^m}\} := \{\sigma_{k_e^m}(r, \hat{v}_{i_1}), \sigma_{k_e^m}(\hat{v}_{i_h}, s), \sigma_{k_e^m}(\hat{v}_{i_j}, \hat{v}_{i_{j+1}}), j = 1, 2, \ldots, h-1\}$, where $\hat{v}_{i_1}, \hat{v}_{i_2}, \ldots, \hat{v}_{i_h}$ is the sequence of battery swapping stations with swapping actions along path $k_e^m$

$B_{k_e^m}$ Set of all the depleting inter-swapping sub-paths along path $k_e^m$ for BEVs in group $m$ between O–D pair $(r, s)$, $B_{k_e^m} := \{\hat{\sigma}_{k_e^m} \in A_{k_e^m} | w[\hat{\sigma}_{k_e^m}] = W_m\}$

$t_a^0$ Free-flow travel time on link$a$

$c_a$ Capacity of link$a$

$c_i$ Service capacity rate of swapping station $i \in I$

$d_i^0$ Free-flow dwell time at battery swapping station $i \in I$

$w_a^0$ Free-flow electricity consumption of link $a$, which is a function of link length and grade.

**Table A.1**
Link capacity (veh/h), free-flow travel time (min) and electricity consumption (kWh).

| Link No. | Tail | Head | Free-flow travel time | Capacity | Electricity consumption |
|---|---|---|---|---|---|
| 1 | 1 | 5 | 17 | 177 | 11 |
| 2 | 1 | 12 | 10 | 104 | 6 |
| 3 | 4 | 5 | 6 | 163 | 4 |
| 4 | 4 | 9 | 16 | 235 | 11 |
| 5 | 5 | 6 | 18 | 245 | 12 |
| 6 | 5 | 9 | 5 | 121 | 3 |
| 7 | 6 | 7 | 8 | 295 | 5 |
| 8 | 6 | 10 | 11 | 213 | 7 |
| 9 | 7 | 8 | 7 | 183 | 4 |
| 10 | 7 | 11 | 8 | 291 | 5 |
| 11 | 8 | 2 | 19 | 275 | 13 |
| 12 | 9 | 10 | 8 | 126 | 5 |
| 13 | 9 | 13 | 6 | 179 | 4 |
| 14 | 10 | 11 | 10 | 241 | 8 |
| 15 | 11 | 2 | 10 | 283 | 7 |
| 16 | 11 | 3 | 11 | 169 | 7 |
| 17 | 12 | 6 | 6 | 164 | 4 |
| 18 | 12 | 8 | 6 | 179 | 4 |
| 19 | 13 | 3 | 10 | 278 | 7 |

**Table A.2**
Feasible path enumeration of GVs and BEVs.

| O–D pair | (1,2) | (1,3) | (4,2) | (4,3) |
|---|---|---|---|---|
| GVs | ⟨1, 5, 6, 7, 8, 2⟩ | ⟨1, 5, 6, 7, 11, 3⟩ | ⟨4, 5, 6, 7, 8, 2⟩ | ⟨4, 5, 6, 7, 11, 3⟩ |
| | ⟨1, 5, 6, 7, 11, 2⟩ | ⟨1, 5, 6, 10, 11, 3⟩ | ⟨4, 5, 6, 7, 11, 2⟩ | |
| | ⟨1, 5, 6, 10, 11, 2⟩ | ⟨1, 5, 9, 10, 11, 3⟩ | | ⟨4, 5, 6, 10, 11, 3⟩ |
| | | | ⟨4, 5, 6, 10, 11, 2⟩ | |
| | ⟨1, 5, 9, 10, 11, 2⟩ | ⟨1, 5, 9, 13, 3⟩ | | |
| | | | | ⟨4, 5, 9, 10, 11, 3⟩ |
| | ⟨1, 12, 6, 7, 8, 2⟩ | ⟨1, 12, 6, 7, 11, 3⟩ | | |
| | | | ⟨4, 5, 9, 10, 11, 2⟩ | |
| | ⟨1, 12, 6, 7, 11, 2⟩ | ⟨1, 12, 6, 10, 11, 3⟩ | | ⟨4, 5, 9, 13, 3⟩ |
| | ⟨1, 12, 6, 10, 11, 2⟩ ⟨1, 12, 8, 2⟩ | | ⟨4, 9, 10, 11, 2⟩ | ⟨4, 9, 10, 11, 3⟩ |
| | | | | ⟨4, 9, 13, 3⟩ |
| BEVs | ⟨1, 5, $\hat{6}$, 7, 8, 2⟩ | ⟨1, 5, $\hat{6}$, 7, 11, 3⟩ | ⟨4, 5, $\hat{6}$, 7, 8, 2⟩ | ⟨4, 5, $\hat{6}$, 7, 11, 3⟩ |
| | ⟨1, 5, $\hat{6}$, 7, 11, 2⟩ | ⟨1, 5, $\hat{6}$, 7, $\hat{11}$, 3⟩ | ⟨4, 5, $\hat{6}$, 7, 11, 2⟩ | |
| | | | | ⟨4, 5, $\hat{6}$, 7, $\hat{11}$, 3⟩ |
| | ⟨1, 5, $\hat{6}$, 7, $\hat{11}$, 2⟩ | ⟨1, 5, $\hat{6}$, 10, 11, 3⟩ | | |
| | | | ⟨4, 5, $\hat{6}$, 7, $\hat{11}$, 2⟩ | |
| | ⟨1, 5, $\hat{6}$, 10, 11, 2⟩ | ⟨1, 5, $\hat{6}$, 10, $\hat{11}$, 3⟩ | | ⟨4, 5, $\hat{6}$, 10, 11, 3⟩ |
| | ⟨1, 5, $\hat{6}$, 10, $\hat{11}$, 2⟩ | ⟨1, 12, $\hat{6}$, 7, 11, 3⟩ | ⟨4, 5, $\hat{6}$, 10, 11, 2⟩ | |
| | | | | ⟨4, 5, $\hat{6}$, 10, $\hat{11}$, 3⟩ |
| | ⟨1, 12, $\hat{6}$, 7, 8, 2⟩ | ⟨1, 12, 6, 7, $\hat{11}$, 3⟩ | | |
| | | | ⟨4, 5, $\hat{6}$, 10, $\hat{11}$, 2⟩ | |
| | ⟨1, 12, $\hat{6}$, 7, 11, 2⟩ | ⟨1, 12, $\hat{6}$, 7, $\hat{11}$, 3⟩ | | ⟨4, 5, 9, 10, $\hat{11}$, 3⟩ |
| | ⟨1, 12, 6, 7, $\hat{11}$, 2⟩ | ⟨1, 12, $\hat{6}$, 10, 11, 3⟩ | | ⟨4, 5, 9, 13, 3⟩ |
| | | | ⟨4, 5, 9, 10, $\hat{11}$, 2⟩ | |
| | ⟨1, 12, $\hat{6}$, 7, $\hat{11}$, 2⟩ | ⟨1, 12, $\hat{6}$, 10, $\hat{11}$, 3⟩ | | ⟨4, 9, 10, $\hat{11}$, 3⟩ |
| | ⟨1, 12, $\hat{6}$, 10, 11, 2⟩ | | ⟨4, 9, 10, $\hat{11}$, 2⟩ | |
| | | | | ⟨4, 9, 13, 3⟩ |
| | ⟨1, 12, $\hat{6}$, 10, $\hat{11}$, 2⟩ | | | |
| | ⟨1, 12, 8, 2⟩ | | | |

**Table A.3**
Equilibrium link flows (veh/h) and swapping flows (veh/h) in Nguyen-Dupius network.

| Link | By path enumeration | By F–W with ML-SBSAPP | Link | By path enumeration | By F–W with ML-SBSAPP |
|---|---|---|---|---|---|
| 1–5 | 703.785 | 703.789 | 9–10 | 324.890 | 324.983 |
| 1–12 | 496.215 | 496.211 | 9–13 | 582.278 | 582.192 |
| 4–5 | 275.110 | 275.218 | 10–11 | 457.749 | 457.860 |
| 4–9 | 524.890 | 524.782 | 11–2 | 537.791 | 537.792 |
| 5–6 | 596.616 | 596.614 | 11–3 | 417.722 | 417.808 |
| 5–9 | 382.278 | 382.393 | 12–6 | 96.215 | 96.5441 |
| 6–7 | 559.972 | 560.281 | 12–8 | 400.000 | 399.666 |
| 6–10 | 132.859 | 132.877 | 13–3 | 582.278 | 582.192 |
| 7–8 | 62.209 | 62.542 | Swapping Node | By path enumeration | By F–W with ML-SBSAPP |
| 7–11 | 497.763 | 497.740 | 6 | 436.107 | 437.910 |
| 8–2 | 462.209 | 462.208 | 11 | 263.893 | 262.257 |

**Table A.4**
Electricity consumption (kW h) of links in Sioux Falls network.

| Link | Electricity consumption | Link | Electricity Consumption | Link | Electricity Consumption | Link | Electricity Consumption |
|---|---|---|---|---|---|---|---|
| 1–2 | 9 | 8–7 | 5 | 13–24 | 6 | 19–17 | 3 |
| 1–3 | 6 | 8–9 | 5 | 14–11 | 6 | 19–20 | 6 |
| 2–1 | 9 | 8–16 | 8 | 14–15 | 8 | 20–18 | 6 |
| 2–6 | 8 | 9–5 | 8 | 14–23 | 6 | 20–19 | 6 |
| 3–1 | 6 | 9–8 | 5 | 15–10 | 9 | 20–21 | 9 |
| 3–4 | 6 | 9–10 | 5 | 15–14 | 8 | 20–22 | 8 |
| 3–12 | 6 | 10–9 | 5 | 15–19 | 6 | 21–20 | 9 |
| 4–3 | 6 | 10–11 | 8 | 15–22 | 6 | 21–22 | 3 |
| 4–5 | 3 | 10–15 | 9 | 16–8 | 8 | 21–24 | 5 |
| 4–11 | 9 | 10–16 | 8 | 16–10 | 8 | 22–15 | 6 |
| 5–4 | 3 | 10–17 | 11 | 16–17 | 3 | 22–20 | 8 |
| 5–6 | 6 | 11–4 | 9 | 16–18 | 5 | 22–21 | 3 |
| 5–9 | 8 | 11–10 | 8 | 17–10 | 11 | 22–23 | 6 |
| 6–2 | 8 | 11–12 | 9 | 17–16 | 3 | 23–14 | 6 |
| 6–5 | 6 | 11–14 | 6 | 17–19 | 3 | 23–22 | 6 |
| 6–8 | 3 | 12–3 | 6 | 18–7 | 3 | 23–24 | 3 |
| 7–8 | 5 | 12–11 | 9 | 18–16 | 5 | 24–13 | 6 |
| 7–18 | 3 | 12–13 | 5 | 18–20 | 6 | 24–21 | 5 |
| 8–6 | 3 | 13–12 | 5 | 19–15 | 6 | 24–23 | 3 |

**Table A.5**
The FFDT (min) and capacity (kW h) at swapping stations.

| Swapping node | FFDT | Capacity |
|---|---|---|
| 5 | 2 | 8000 |
| 11 | 1.5 | 10,000 |
| 15 | 1 | 8000 |
| 16 | 2 | 2000 |

**Table A.6**
Equilibrium link flow (veh/h) in Sioux Falls network.

| Link | Flow | Link | Flow | Link | Flow | Link | Flow |
|---|---|---|---|---|---|---|---|
| 1–2 | 2600 | 8–7 | 12,164 | 13–24 | 9671 | 19–17 | 16,665 |
| 1–3 | 6900 | 8–9 | 12,222 | 14–11 | 13,454 | 19–20 | 9557 |
| 2–1 | 2450 | 8–16 | 10,557 | 14–15 | 8865 | 20–18 | 12,359 |
| 2–6 | 5700 | 9–5 | 8407 | 14–23 | 9009 | 20–19 | 5523 |
| 3–1 | 7050 | 9–8 | 11,351 | 15–10 | 18,886 | 20–21 | 6500 |
| 3–4 | 13,200 | 9–10 | 23,738 | 15–14 | 8734 | 20–22 | 11,717 |
| 3–12 | 7320 | 10–9 | 23,966 | 15–19 | 11,525 | 21–20 | 5850 |
| 4–3 | 12,817 | 10–11 | 18,176 | 15–22 | 17,561 | 21–22 | 10,569 |
| 4–5 | 16,503 | 10–15 | 20,922 | 16–8 | 9835 | 21–24 | 12,329 |
| 4–11 | 7106 | 10–16 | 11,661 | 16–10 | 12,861 | 22–15 | 20,484 |
| 5–4 | 15,841 | 10–17 | 8483 | 16–17 | 12,531 | 22–20 | 8684 |
| 5–6 | 11,446 | 11–4 | 7486 | 16–18 | 11,042 | 22–21 | 10,629 |
| 5–9 | 7407 | 11–10 | 17,692 | 17–10 | 9933 | 22–23 | 11,471 |
| 6–2 | 5550 | 11–12 | 10,502 | 17–16 | 12,238 | 23–14 | 9105 |
| 6–5 | 9783 | 11–14 | 13,490 | 17–19 | 15,509 | 23–22 | 11,421 |
| 6–8 | 17,885 | 12–3 | 7853 | 18–7 | 9061 | 23–24 | 5606 |
| 7–8 | 11,944 | 12–11 | 10,534 | 18–16 | 11,813 | 24–13 | 10,235 |
| 7–18 | 9281 | 12–13 | 12,271 | 18–20 | 11,908 | 24–21 | 11,619 |
| 8–6 | 16,073 | 13–12 | 12,936 | 19–15 | 6334 | 24–23 | 5652 |

**Table A.7**
Scenarios with respect to the number of swapping stations.

| Scenario | Swapping node | FFDT | Capacity |
|---|---|---|---|
| NumStation = 4 | 5 | 2 | 8000 |
| | 11 | 1.5 | 10,000 |
| | 15 | 1 | 8000 |
| | 16 | 2 | 2000 |
| NumStation = 6 | 5 | 2 | 8000 |
| | 6 | 2 | 8000 |
| | 11 | 1.5 | 10,000 |
| | 15 | 1 | 8000 |
| | 16 | 2 | 2000 |
| | 23 | 1 | 8000 |
| NumStation = 8 | 4 | 2 | 8000 |
| | 5 | 2 | 8000 |
| | 6 | 2 | 8000 |
| | 11 | 1.5 | 10,000 |
| | 15 | 1 | 8000 |
| | 16 | 2 | 2000 |
| | 19 | 2 | 2000 |
| | 23 | 1 | 8000 |

**Table A.8**
Scenarios with respect to the deployment of swapping stations.

| Scenario | Station | Swapping node | FFDT | Capacity |
|---|---|---|---|---|
| Deployment 1 | Station #1 | 5 | 2 | 8000 |
| | Station #2 | 11 | 1.5 | 10,000 |
| | Station #3 | 15 | 1 | 8000 |
| | Station #4 | 16 | 2 | 2000 |
| Deployment 2 | Station #1 | 4 | 2 | 8000 |
| | Station #2 | 8 | 1 | 8000 |
| | Station #3 | 19 | 2 | 2000 |
| | Station #4 | 24 | 1.5 | 10,000 |
| Deployment 3 | Station #1 | 6 | 2 | 8000 |
| | Station #2 | 10 | 1.5 | 10,000 |
| | Station #3 | 19 | 2 | 2000 |
| | Station #4 | 23 | 1 | 8000 |

**Table A.9**
Link capacity (veh/h), free-flow travel time (min) and electricity consumption (kW h).

| Link No. | Tail | Head | Free-flow travel time | Capacity | Free-flow electricity consumption |
|---|---|---|---|---|---|
| 1 | 1 | 4 | 15.0 | 300 | 3.25 |
| 2 | 1 | 5 | 7.0 | 100 | 0.75 |
| 3 | 1 | 7 | 15.0 | 200 | 5.50 |
| 4 | 2 | 1 | 11.0 | 100 | 0.75 |
| 5 | 2 | 6 | 2.5 | 200 | 0.75 |
| 6 | 3 | 4 | 4.0 | 200 | 3.50 |
| 7 | 3 | 7 | 12.0 | 100 | 2.50 |
| 8 | 4 | 7 | 5.0 | 600 | 3.43 |
| 9 | 5 | 7 | 2.0 | 200 | 3.00 |
| 10 | 6 | 5 | 3.5 | 150 | 0.75 |
| 11 | 6 | 7 | 17.4 | 300 | 4.20 |

**Table A.10**
Equilibrium link flows (veh/h) in Yang–Bell network.

| Link | Solution 1 | Solution 2 | Link | Solution 1 | Solution 2 |
|---|---|---|---|---|---|
| 1–4 | 300 | 310 | 3–7 | 200 | 210 |
| 1–5 | 200 | 170 | 4–7 | 600 | 600 |
| 1–7 | 300 | 300 | 5–7 | 500 | 485 |
| 2–1 | 200 | 180 | 6–5 | 300 | 315 |
| 2–6 | 300 | 320 | 6–7 | 400 | 405 |
| 3–4 | 300 | 290 | | | |

**Table A.11**
Equilibrium path flows (veh/h) and travel cost (min) of GVs in Yang–Bell network.

| | O–D pair | Path | Path flow | Travel cost |
|---|---|---|---|---|
| Solution 1 | (1,7) | 1,4,7 | 300 | 23.0 |
| | (2,7) | 2,6,5,7 | 250 | 30.0 |
| | (3,7) | 3,4,7 | 250 | 12.8 |
| | (6,7) | 6,7 | 200 | 25.6 |
| Solution 2 | (1,7) | 1,4,7 | 300 | 23.3 |
| | (2,7) | 2,6,5,7 | 245 | 31.0 |
| | | 267 | 5 | 31.0 |
| | (3,7) | 3,4,7 | 250 | 12.4 |
| | (6,7) | 6,7 | 200 | 26.1 |

**Table A.12**
Equilibrium path flows (veh/h) and travel cost (min) of BEVs in Yang–Bell network.

| | O–D pair | Path | Path flow | Travel cost | Sub-path | Electricity consumption |
|---|---|---|---|---|---|---|
| Solution 1 | (1,7) | 1,7 | 300 | 26.4 | 1,7 | 22 |
| | (2,7) | 2,6,5,7 | 50 | 30.0 | 2,6,5,7 | 24 |
| | | 2,1,5,7 | 200 | 74.9 | 2,1,5,7 | 24 |
| | (3,7) | 3,4,7 | 50 | 12.8 | 3,4 | 14 |
| | | | | | 4,7 | 24 |
| | | 3,7 | 200 | 41 | 3,7 | 8 |
| | (6,7) | 6,7 | 200 | 25.6 | 6,7 | 21 |
| Solution 2 | (1,7) | 1,4,7 | 10 | 23.3 | 1,4 | 13 |
| | | | | | 4,7 | 24 |
| | | 1,7 | 290 | 26.4 | 1,7 | 22 |
| | (2,7) | 2,1,5,7 | 170 | 56.5 | 2,1,5,7 | 20 |
| | | 2,1,7 | 10 | 54.7 | 2,1,7 | 24 |
| | | 2,6,5,7 | 70 | 31.0 | 2,6,5,7 | 24 |
| | (3,7) | 3,4,7 | 40 | 12.4 | 3,4 | 14 |
| | | | | | 4,7 | 24 |
| | | 3,7 | 210 | 47.0 | 3,7 | 8 |
| | (6,7) | 6,7 | 200 | 26.1 | 6,7 | 21 |

## References


Adler, J.D., Mirchandani, P.B., Xue, G., Xia, M., 2016. The electric vehicle shortest-walk problem with battery exchanges. Netw. Spat. Econ. 16 (1), 155–173.
Adler, J.D., Mirchandani, P.B., 2014. Online routing and battery reservations for electric vehicles with swappable batteries. Transp. Res. Part B 70, 285–302.
Aneja, Y.P., Aggarwal, V., Nair, K.P.K., 1983. Shortest chain subject to side constraints. Networks 13, 295–302.
Ban, J.X., Liu, H.X., Ferris, M.C., Ran, B., 2006. A general MPCC model and its solution algorithm for continuous network design problem. Math. Comp. Modell. 43 (5), 493–505.
Bar-Gera, H., 2013. Transportation network test problems http://www.bgu.ac.il/~bargera/tntp/ (accessed 19.06.15)
Berr, D., 2008. Investigation into the Scope for the Transport Sector to Switch to Electric Vehicles and Plugin Hybrid Vehicles.
Bigazzi, A.Y., Clifton, K.J., 2015. Modeling the effects of congestion on fuel economy for advanced power train vehicles. Transp. Plann. Tech. 38, 149–161.
Cabral, E.A., 2005. Wide Area Telecommunication Network Design: Problems and Solution Algorithms with Application to the Alberta Supernet. University of Alberta, p. 109.
Chan, C.C., 2007. The State of the Art of Electric, Hybrid, and Fuel Cell Vehicles. Proceedings of the IEEE 95, 704–718.
Charles Botsford, A.S., 2009. Fast charging vs. slow charging: Pros and cons for the new age of electric vehicles. International Battery, Hybrid and Fuel Cell Electric Vehicle Symposium and Exhibition, EVS.
Daganzo, C.F., Sheffi, Y., 1977. On stochastic models of traffic assignment. Transp. Sci. 11 (3), 253–274.
Di, X., Liu, H.X., 2016. Boundedly rational route choice behavior: A review of models and methodologies. Transp. Res. Part B 85, 142–179.
Di, X., Liu, H.X., Pang, J.S., Ban, X.J., 2013. Boundedly rational user equilibria (BRUE): mathematical formulation and solution sets. Transp. Res. Part B. 57, 300–313.
Dijkstra, E.W., 1959. A note on two problems in connexion with graphs. Numer. Math. 1, 269–271.
Dumitrescu, I., Boland, N., 2003. Improved preprocessing, labeling and scaling algorithms for the Weight-Constrained Shortest Path Problem. Networks 42, 135–153.
Duvall, M., Knipping, E., Alexander, M., Tonachel, L., Clark, C., 2007. Environmental Assessment Of Plug-In Hybrid Electric Vehicles.
Eberle, D.U., von Helmolt, D.R., 2010. Sustainable transportation based on electric vehicle concepts: a brief overview. Energy Environ. Sci. 3, 689–699.
Egbue, O., Long, S., 2012. Barriers to widespread adoption of electric vehicles: an analysis of consumer attitudes and perceptions. Energy Policy 48, 717–729.
Electric Car (EC), 2007. Unlimited range electric car https://www.youtube.com/watch?gl=SG&hl=en-GB&v=M0SB5psrVCM (accessed 13.6.15)
Electric Transportation Engineering Corporation (ETEC), 2010. Electric Vehicle Charging Infrastructure Deployment Guidelines for the State of Tennessee.
Franke, T., Neumann, I., Bühler, F., Cocron, P., Krems, J.F., 2012. Experiencing Range in an Electric Vehicle: Understanding Psychological Barriers. Appl. Psychol. 61, 368–391.
Frey, H.C., Zhang, K., Rouphail, N.M., 2008. Fuel Use and Emissions Comparisons for Alternative Routes, Time of Day, Road Grade, and Vehicles Based on In-Use Measurements. Environ. Sci.Technol. 42, 2483–2489.
Ghamami, M., Zockaie, A., Nie, Y.M., 2016. A general corridor model for designing plug-in electric vehicle charging infrastructure to support intercity travel. Transp. Res Part C 68, 389–402.
He, F., Wu, D., Yin, Y., Guan, Y., 2013. Optimal deployment of public charging stations for plug-in hybrid electric vehicles. Transp. Res. Part B 47, 87–101.
He, F., Yin, Y., Lawphongpanich, S., 2014. Network equilibrium models with battery electric vehicles. Transp. Res. Part B 67, 306–319.
He, F., Yin, Y., Zhou, J., 2015. Deploying public charging stations for electric vehicles on urban road networks. Transp. Res Part C 60, 227–240.
Jiang, N., Xie, C., 2014. Computing and Analyzing Mixed Equilibrium Network Flows with Gasoline and Electric Vehicles. Comput.-Aided Civ. Infrastruct. Eng. 29, 626–641.
Jiang, N., Xie, C., Duthie, J.C., Waller, S.T., 2014. A network equilibrium analysis on destination, route and parking choices with mixed gasoline and electric vehicular flows. EURO J. Transp. Logistics 3, 55–92.
Jiang, N., Xie, C., Waller, S., 2012. Path-Constrained Traffic Assignment. Transp. Res. Rec. 2283, 25–33.
Jing, W., Yan, Y., Kim, I., Sarvi, M., 2016. Electric vehicles: A review of network modelling and future research needs. Adv. Mech. Eng. 8 (1) 1687814015627981.
Kendall, D.G., 1953. Stochastic Processes Occurring in the Theory of Queues and their Analysis by the Method of the Imbedded Markov Chain. Ann. Math. Stat. 24, 338–354.
Laporte, G., Pascoal, M.M.B., 2011. Minimum cost path problems with relays. Comput. Oper. Res. 38, 165–173.
Li, S., Huang, Y., Mason, S.J., 2016. A multi-period optimization model for the deployment of public electric vehicle charging stations on network. Transp. Res. Part C 65, 128–143.
Liao, C.S., Lu, S.H., Shen, Z.J.M., 2016. The electric vehicle touring problem. Transp. Res. Part B 86, 163–180.
Little, J.D.C., 1961. A Proof for the Queuing Formula: $L = \lambda W$. Oper. Res. 9, 383–387.
Liu K., Yamamoto T. and Morikawa T., Impact of road gradient on energy consumption of electric vehicles, 2015. working paper.
Lou, Y., Yin, Y., Lawphongpanich, S., 2010. Robust congestion pricing under boundedly rational user equilibrium. Transp. Res. Part B 44 (1), 15–28.
Mak, H.-Y., Rong, Y., Shen, Z.-J.M., 2013. Infrastructure planning for electric vehicles with battery swapping. Manage. Sci. 59, 1557–1575.
Meng, Q., Liu, Z., 2012. Mathematical models and computational algorithms for probit-based asymmetric stochastic user equilibrium problem with elastic demand. Transportmetrica 8 (4), 261–290.
Meng, Q., Liu, Z., Wang, S., 2012. Optimal distance tolls under congestion pricing and continuously distributed value of time. Transp. Res. Part E 48 (5), 937–957.
Nguyen, S., Dupuis, C., 1984. An Efficient Method for computing traffic equilibria in networks with asymmetric transp. costs. Transp. Sci. 18, 185–202.
Nie, Y.M., Ghamami, M., 2013. A corridor-centric approach to planning electric vehicle charging infrastructure. Transp. Res. Part B 57, 172–190.
Nissan, 2016. http://www.nissanusa.com/electric-cars/leaf/ (accessed 12.02.16)
NTU, 2014. Ultra-fast charging batteries that can be 70% recharged in just two minutes Science Daily https://www.sciencedaily.com/releases/2014/10/141013090449.htm (accessed 05.02.16)
Pearre, N.S., Kempton, W., Guensler, R.L., Elango, V.V., 2011. Electric vehicles: How much range is required for a day's driving? Transp. Res. Part C 19, 1171–1184.
Sathaye, N., Kelley, S., 2013. An approach for the optimal planning of electric vehicle infrastructure for highway corridors. Transp. Res. Part E 59, 15–33.
Schneider, M., Stenger, A., Goeke, D., 2014. The electric vehicle-routing problem with time windows and recharging stations. Transp. Science 48, 500–520.
Smith, O.J., Boland, N., Waterer, H., 2012. Solving shortest path problems with a weight constraint and replenishment arcs. Comput. Oper. Res. 39, 964–984.
Travesset-Baro, O., Rosas-Casals, M., Jover, E., 2015. Transport energy consumption in mountainous roads. A comparative case study for internal combustion engines and electric vehicles in Andorra. Transp. Res. Part D 34, 16–26.
Wang, S., Meng, Q., Yang, H., 2013. Global optimization methods for the discrete network design problem. Transp. Res. Part B 50, 42–60.
Wardrop, J.G., 1952. Some theoretical aspects of road traffic research. In: Proceedings, Institution of Civil Engineers II (1), pp. 325–378.
Yabe, K., Shinoda, Y., Seki, T., Tanaka, H., Akisawa, A., 2012. Market penetration speed and effects on $CO_2$ reduction of electric vehicles and plug-in hybrid electric vehicles in Japan. Energy Policy 45, 529–540.
Yang, H., Bell, M.G., 1997. Traffic restraint, road pricing and network equilibrium. Transp. Res. Part B 31, 303–314.
Yang, H., Bell, M.G., 1998. Models and algorithms for road network design: a review and some new developments. Transp. Rev. 18 (3), 257–278.
Yang, H., Huang, H.J., 2005. Mathematical and Economic Theory of Road Pricing. Elsevier.
Zhang, B., 2015. Tesla's battery swapping plan is a mere shadow of the promise it once showed Business Insider http://www.businessinsider.sg/teslas-battery-swapping-plan-isnt-working-out-2015-6/?r=US&IR=T#.V3EVxPkQiMU (accessed 02.01.16)